

# Neuroserpin alleviates cerebral ischemia-reperfusion injury by suppressing ischemia-induced endoplasmic reticulum stress

Yumei Liao<sup>1,2,3,#</sup>, Qinghua Zhang<sup>3,#</sup>, Qiaoyun Shi<sup>3,#</sup>, Peng Liu<sup>2,3</sup>, Peiyun Zhong<sup>3</sup>, Lingling Guo<sup>2,3</sup>, Zijian Huang<sup>2,3</sup>, Yinghui Peng<sup>2,3</sup>, Wei Liu<sup>4</sup>, Shiqing Zhang<sup>2,3</sup>, István Adorján<sup>5</sup>, Yumi Fukuzaki<sup>6</sup>, Eri Kawashita<sup>7</sup>, Xiao-Qi Zhang<sup>2,3</sup>, Nan Ma<sup>2,\*</sup>, Xiaoshen Zhang<sup>1,8,\*</sup>, Zoltán Molnár<sup>9,\*</sup>, Lei Shi<sup>1,2,3,\*</sup>

<https://doi.org/10.4103/NRR.NRR-D-24-00044>

Date of submission: January 11, 2024

Date of decision: May 6, 2024

Date of acceptance: June 6, 2024

Date of web publication: September 6, 2024

## From the Contents

Introduction

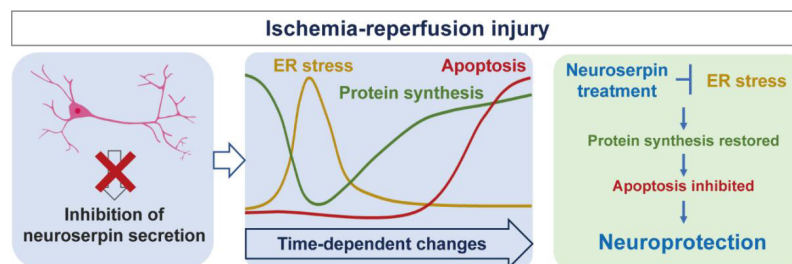
Methods

Results

Discussion

## Graphical Abstract

*A novel mechanism of the neuroprotective properties of neuroserpin*



## Abstract

Neuroserpin, a secreted protein that belongs to the serpin superfamily of serine protease inhibitors, is highly expressed in the central nervous system and plays multiple roles in brain development and pathology. As a natural inhibitor of recombinant tissue plasminogen activator, neuroserpin inhibits the increased activity of tissue plasminogen activator in ischemic conditions and extends the therapeutic windows of tissue plasminogen activator for brain ischemia. However, the neuroprotective mechanism of neuroserpin against ischemic stroke remains unclear. In this study, we used a mouse model of middle cerebral artery occlusion and oxygen-glucose deprivation/reperfusion-injured cortical neurons as *in vivo* and *in vitro* ischemia-reperfusion models, respectively. The models were used to investigate the neuroprotective effects of neuroserpin. Our findings revealed that endoplasmic reticulum stress was promptly triggered following ischemia, initially manifesting as the acute activation of endoplasmic reticulum stress transmembrane sensors and the suppression of protein synthesis, which was followed by a later apoptotic response. Notably, ischemic stroke markedly downregulated the expression of neuroserpin in cortical neurons. Exogenous neuroserpin reversed the activation of multiple endoplasmic reticulum stress signaling molecules, the reduction in protein synthesis, and the upregulation of apoptotic transcription factors. This led to a reduction in neuronal death induced by oxygen/glucose deprivation and reperfusion, as well as decreased cerebral infarction and neurological dysfunction in mice with middle cerebral artery occlusion. However, the neuroprotective effects of neuroserpin were markedly inhibited by endoplasmic reticulum stress activators thapsigargin and tunicamycin. Our findings demonstrate that neuroserpin exerts neuroprotective effects on ischemic stroke by suppressing endoplasmic reticulum stress.

**Key Words:** endoplasmic reticulum stress; ischemia-reperfusion injury; neuron; neuronal apoptosis; neuroprotection; neuroserpin; protein synthesis; secretory protein; stroke; transcriptomic analysis

<sup>1</sup>Department of Cardiovascular Surgery, The First Affiliated Hospital, Jinan University, Guangzhou, Guangdong Province, China; <sup>2</sup>State Key Laboratory of Bioactive Molecules and Druggability Assessment, Jinan University, Guangzhou, Guangdong Province, China; <sup>3</sup>JNU-HKUST Joint Laboratory for Neuroscience and Innovative Drug Research; Guangdong Province Key Laboratory of Pharmacodynamic Constituents of TCM and New Drugs Research, College of Pharmacy, Jinan University, Guangzhou, Guangdong Province, China; <sup>4</sup>Shenzhen Key Laboratory for Neuronal Structural Biology, Biomedical Research Institute; Institute of Geriatric Medicine, Peking University Shenzhen Hospital, Shenzhen Peking University-The Hong Kong University of Science and Technology Medical Center, Shenzhen, Guangdong Province, China; <sup>5</sup>Department of Anatomy, Histology and Embryology, Semmelweis University, Budapest, Hungary; <sup>6</sup>Department of Neurology, University of California, San Francisco, San Francisco, CA, USA; <sup>7</sup>Department of Pathological Biochemistry, Kyoto Pharmaceutical University, Yamashina-ku, Kyoto, Japan; <sup>8</sup>School of Nursing, Jinan University, Guangzhou, Guangdong Province, China; <sup>9</sup>Department of Physiology, Anatomy and Genetics, University of Oxford, Oxford, UK

\*Correspondence to: Nan Ma, PhD, nanma927@126.com; Xiaoshen Zhang, MD, PhD, xsh.zhang@hotmail.com; Zoltán Molnár, MD, DPhil, zoltan.molnar@dpag.ox.ac.uk; Lei Shi, PhD, t\_shilei@jnu.edu.cn or sophielshi80@gmail.com.

<https://orcid.org/0000-0002-8518-5627> (Nan Ma); <https://orcid.org/0009-0005-5473-2631> (Xiaoshen Zhang); <https://orcid.org/0000-0002-6852-6004> (Zoltán Molnár);

<https://orcid.org/0000-0001-8695-3432> (Lei Shi)

#These authors contributed equally to this work and share first authorship.

**Funding:** This study was supported in part by the National Key Research & Development Program of China, No. 2022YFA1104900 (to LS); the National Natural Science Foundation of China, Nos. 82371175, 82071535 (both to LS), 82101614 (to YP); the International Science and Technology Cooperation Projects of Guangdong Province, No. 2023A0505050121 (to LS); Guangdong Basic and Applied Basic Research Foundation, Nos. 2022B1515130007 (to LS), 2023A1515030012 (to SZ), 2022A1515010666 (to WL); the Science and Technology Program of Guangzhou, Nos. 202102070001 (to LS), 202201010041 (to YP); and Shenzhen Basic Research Grant, Nos. JCYJ20200109140414636, JCYJ20230807145103007 (both to WL). Lei Shi was awarded a Royal Society Newton Advanced Fellowship, No. AOMS-NAF0051003, in collaboration with Zoltán Molnár, Department of Physiology, Anatomy and Genetics, University of Oxford (2017–2021).

**How to cite this article:** Liao Y, Zhang Q, Shi Q, Liu P, Zhong P, Guo L, Huang Z, Peng Y, Liu W, Zhang S, Adorján I, Fukuzaki Y, Kawashita E, Zhang XQ, Ma N, Zhang X, Molnár Z, Shi L (2026) Neuroserpin alleviates cerebral ischemia-reperfusion injury by suppressing ischemia-induced endoplasmic reticulum stress. *Neural Regen Res* 21(1):333-345.



## Introduction

During ischemic stroke, prolonged ischemia leads to a lack of glucose and oxygen in brain tissues, resulting in anaerobic metabolism and the subsequent decrease of ATP levels and cellular pH, causing dysfunction of ion transport mechanisms and intracellular calcium overload and eventually inducing neuronal death via apoptotic/autophagic/necrotic mechanisms (Mayer and Miller, 1990; Lee et al., 2000; Kalogeris et al., 2012). Currently, the main therapeutic strategy is to restore the blood flow for tissue reperfusion within a narrow time window after ischemia, which is achieved by intravenous thrombolysis with recombinant tissue plasminogen activator (tPA) or endovascular thrombectomy (National Institute of Neurological Disorders and Stroke rt-PA Stroke Study Group, 1995; Campbell et al., 2019). While reperfusion restores oxygen and nutrition, the enhanced generation of reactive oxygen species exacerbates the intracellular dysfunction such as intracellular calcium overload, triggering delayed neuronal death and increased cerebral infarct volume (Kalogeris et al., 2012; George and Steinberg, 2015). Therefore, better understanding of the mechanisms by which ischemia-reperfusion (I/R) causes neuronal injury may lead to the development of therapeutic strategies.

Endoplasmic reticulum (ER), a pivotal organelle for protein synthesis and cellular homeostasis, is sensitive to various stress stimuli (Almanza et al., 2019). Growing experimental evidence from *in vivo* middle cerebral artery occlusion (MCAO) and *in vitro* oxygen-glucose deprivation (OGD) models indicates that I/R activates ER stress, also known as the unfolded protein response, which triggers neuronal apoptosis (Xin et al., 2014; Thiebaut et al., 2019; Han et al., 2021b; Wang et al., 2022). Once ischemia or OGD occurs, the ER becomes dysfunctional and abundant unfolded proteins accumulate in the ER lumen to trigger the ER stress response (Tang et al., 2024). At least three signaling pathways are known to induce ER stress-mediated cellular responses including protein synthesis inhibition and apoptosis. Each signaling axis is initiated by one of the following transmembrane sensors: double-stranded RNA-activated protein kinase-like ER kinase (PERK), inositol requiring enzyme 1 (IRE1), or activating transcription factor 6 (ATF6) (Walter and Ron, 2011). PERK activation leads to inhibition of protein synthesis to relieve the protein folding load of ER; it also promotes activating transcription factor 4 (ATF4)-dependent transcription of pro-apoptotic factors including CCAAT/enhancer binding protein homologous protein (CHOP) (Badiola et al., 2011; Walter and Ron, 2011; Roussel et al., 2013). Both regulations are through inhibition of eukaryotic translation initiation factor 2 $\alpha$  (eIF2 $\alpha$ ) by PERK-mediated phosphorylation. ER stress inhibitors were shown to alleviate neuronal apoptosis and cerebral injury (Nakka et al., 2010; Srinivasan and Sharma, 2011), suggesting that the ER may be a potential therapeutic target for neuroprotection. However, the temporal profiles of different signaling molecules of ER stress and apoptosis during I/R are unknown. Understanding the sequence and causal relations of different signaling events, especially during the early stages of I/R (minutes to 24 hours after ischemia), will provide critical information for the time window of possible therapeutic intervention.

Neuroserpin, a secreted protein that belongs to the serpin superfamily of serine protease inhibitors, is highly expressed in the central nervous system and plays multiple roles in brain development and pathology (Krueger et al., 1997; Lee et al., 2017; Adorjan et al., 2019; Ding et al., 2021; Godinez et al., 2022; Satapathy and Wilson, 2023). Evidence has shown that neuroserpin has neuroprotective effects against ischemic and hemorrhagic brain damage (Millar et al., 2017; Ding et al., 2021). Higher levels of serum neuroserpin at the onset of cerebral ischemia are associated with a smaller infarct volume and better outcome for patients (Rodríguez-González et al., 2011c; Wu et al., 2017). In rodent models, the application of neuroserpin reduces neuronal apoptosis and cerebral infarct volume caused by MCAO (Yepes et al., 2000; Cinelli et al., 2001), whereas neuroserpin-deficient mice display a worse cerebral injury and neurological outcome (Gelderblom et al., 2013). Neuroserpin also displays neuroprotective effects in OGD/reperfusion (OGD/R) cell models (Rodríguez-González et al., 2011a; Yang et al., 2016). As an inhibitor of tPA, neuroserpin inhibits the increased tPA activity in ischemic conditions (Yepes et al., 2000; Rodríguez-González et al., 2011a). This is considered one of the main mechanisms of its neuroprotective effects. Neuroserpin also alleviates ischemic infarct volume, blood-brain barrier damage, and neuron apoptosis caused by prolonged treatment of tPA thrombolysis in MCAO rat models, suggesting that it may extend the therapeutic windows of tPA for brain ischemia (Zhang et al., 2002; Cai et al., 2020). Additionally, multiple studies demonstrated that neuroserpin exhibits neuroprotective effects against ischemia-induced neuronal death in

tPA-deficient mice and neurons, indicating tPA-independent mechanisms (Wu et al., 2010; Ma et al., 2012; Gu et al., 2015). However, the neuroprotective mechanisms of neuroserpin are not fully understood, and whether neuroserpin exerts its effects through altering the ER stress response has not been explored.

In the present study, we explored the temporal profile of signaling events of ER stress and apoptosis during the first 24 hours of reperfusion after ischemia using the models of MCAO-injured mice and OGD/R-injured cortical neurons. We further investigated the therapeutic effect and mechanism of neuroserpin. These results may provide novel mechanistic insights and ER-targeting therapeutic strategies for ischemic stroke.

## Methods

### Animals

Male adult C57BL/6J mice (weighing 20–25 g, 8–10 weeks of age,  $n = 100$ ), purchased from Beijing HFK Bioscience Co., Ltd. (Beijing, China; license No. SCXK (Jing) 2014-0004), were used to establish the sham/MCAO model. Male mice were used because they exhibit more consistent and reproducible infarct sizes compared with females, and the hormonal fluctuations in female mice might result in additional variability in experimental outcomes. Mice were housed at 3–5 mice per cage in an environment of  $25 \pm 1^\circ\text{C}$  and 50% relative humidity, with a 12-hour light/12-hour dark cycle (light on from 8:00 to 20:00) and *ad libitum* access to food and water.

Mice were randomly assigned to the experimental groups: sham surgery, MCAO surgery, or treatment of neuroserpin and/or ER stress activators. Each experimental group contained 3–11 mice (3–5 for western blot analysis and RNA sequencing analysis, 6–11 for evaluation of neurological score and infarction area).

Seven pregnant Sprague-Dawley rats (gestational age 18.5 days), purchased from the Institute of Laboratory Animals at Southern Medical University, China (license No. SCXK (Yue) 2016-0041), were used for the preparation of primary neuronal cultures.

All animal experiments were approved by the Animal Care and Use Committee of the animal facility at Jinan University, China (approval Nos. IACUC-20210330-15 and IACUC-20220407-02) on September 12, 2022 and the Institutional Animal Care and Use Committee of Guangzhou Ruige Biotechnology, China (approval No. IACUC-20230210-018) on February 10, 2023. All experiments were designed and reported following the Animal Research: Reporting of *In Vivo* Experiments (ARRIVE) guidelines (Percie du Sert et al., 2020).

### Establishment of the transient middle cerebral artery occlusion model

Transient MCAO was performed following published protocols (Hu et al., 2021; Pan et al., 2022). Briefly, mice were anesthetized by inhalation of 3% isoflurane (RWD Life Science Co., Ltd., Shenzhen, China, Cat# R510-22-10) for induction and 1% isoflurane for maintenance. The skin of the neck was disinfected with 75% alcohol and a cut was made along the middle of the neck, exposing the cervical blood vessels. The right common carotid artery, external carotid artery, and internal carotid artery were carefully dissected from surrounding tissues and nerves. The external carotid artery, common carotid artery, and internal carotid artery were ligated with 6-0 silk sutures or hemostatic clips. A small incision was made in the external carotid artery followed by insertion of a standardized silicone rubber-coated 6-0 nylon monofilament (Yushun Biotech, Guangzhou, China) through the external carotid artery into the internal carotid artery to block the origin of the middle cerebral artery. After 1.5 hours, the mice were re-anesthetized, the filament was withdrawn, the common carotid artery was loosened to allow reperfusion, and the incision was sutured. The sham group was anesthetized and the neck blood vessels were exposed as in the same way as MCAO group; the incision was sutured at 1.5 hours after the sham surgery. The body temperature of mice was maintained at  $37 \pm 0.5^\circ\text{C}$  by placing them on a heating pad during the surgery.

### Assessment of neurological function

Neurological function was assessed by Zea-Longa test (Longa et al., 1989) 24 hours after MCAO by a graded score of 0 to 4. No neurological deficit was scored as 0; failure to extend the contralateral forepaw was scored as 1; contralateral rotation during walking was scored as 2; leaning to the contralateral side was scored as 3; and failure to walk spontaneously was scored as 4.

### Measurement of cerebral infarction

The infarct volume was measured in serial coronal sections of the brains stained with 2,3,5-triphenyl-tetrazolium chloride (Sigma-Aldrich, Burlington, MA, USA) (Zhang et al., 2021; Zhao et al., 2022). The brains were collected and frozen at  $-20^{\circ}\text{C}$  for 20 minutes and then coronally sliced into 1.5 mm slices. The slices were incubated with 0.2% 2,3,5-triphenyl-tetrazolium chloride in Dulbecco's phosphate-buffered saline for 30 minutes at  $37^{\circ}\text{C}$ , followed by fixation with 4% paraformaldehyde (Sigma-Aldrich). After scanning and digitizing, the infarct area (%) in each slice was calculated by the following formula: (the contralateral hemisphere area – the non-infarct area in the ipsilateral hemisphere)/contralateral hemisphere area  $\times$  100. The infarct volume (%) of each brain was calculated as the average infarct area of all slices (Gong et al., 2017).

### Primary cortical neuronal culture

Primary cortical neurons were cultured as described previously (Guo et al., 2021; Liao et al., 2023). Briefly, pregnant Sprague–Dawley rats (gestational age 18.5 days) were lightly anesthetized with 3% isoflurane followed by cervical dislocation. The cortices from the embryos were dissected out in ice-cold calcium, magnesium, bicarbonate-free Hank's balanced salt solution (Life Technologies, Waltham, MA, USA) and digested in 0.05% trypsin at  $37^{\circ}\text{C}$  for 20 minutes. Cells were dissociated by pipetting 15–20 times in the plating media (Dulbecco's modified Eagle medium containing 5% horse serum and 1% penicillin-streptomycin) and plated on poly-L-lysine (Sigma-Aldrich, 0.1 mg/mL)-coated culture dishes ( $8 \times 10^5$  cells/35 mm dish), 12-well plates ( $6 \times 10^4$  cells/18 mm coverslip), or 96-well plates ( $1 \times 10^5$ /well). Cells were cultured in Neurobasal medium (Gibco, Carlsbad, NM, USA, Cat# 21103049) supplemented with 2% B27, 1 mM L-glutamine, 10 mM D-glucose, and 1% penicillin-streptomycin (Life Technologies). Primary cortical neurons were identified by immunoreactivity of microtubule-associated protein 2 (MAP2), a neuronal marker. All neuronal culture experiments were repeated at least three times.

### Oxygen-glucose deprivation reperfusion model establishment and treatments

Cortical neurons were damaged by OGD/R at 7 days *in vitro* (DIV) (Shi et al., 2019). Cells were maintained in Dulbecco's modified Eagle medium without glucose (Life Technologies) and placed in a hypoxia chamber (Billups-Rothenberg, Del Mar, CA, USA) with premixed gas (95%  $\text{N}_2$  and 5%  $\text{CO}_2$ ) for 4 hours. The cells were then incubated in standard culture medium under normoxic conditions for another 24 hours. The medium or cell lysates were collected after the 4-hour OGD phase and different time points after reperfusion. As a control, cortical neurons (7 DIV) were changed to new standard medium and cultured under normoxic conditions for 4 hours, and the medium or cell lysates were collected.

For investigating the possible protective effect of secreted neuroserpin, the medium collected from the control neurons was used as the conditioned medium for application in OGD-injured neurons for the reperfusion phase. To neutralize the secreted neuroserpin, anti-neuroserpin antibody (50 ng for 20,000 cells, Santa Cruz Biotechnology, Dallas, TX, USA, Cat# sc-48360, RRID:AB\_628245) was added to the conditional medium.

For neuroserpin and drug treatment in cultured neurons, recombinant non-glycosylated human neuroserpin (1–100 ng/mL, PeproTech, Cranbury, NJ, USA, Cat# 130-14, produced in *Escherichia coli*) was added for 4 hours before OGD or immediately after reperfusion. The ER stress inhibitors sodium 4-phenylbutyrate (4-PBA, 50 and 100  $\mu\text{M}$ , Selleck, Houston, TX, USA) and salubrinal (25 and 100  $\mu\text{M}$ , Selleck) were added for 1 hour before OGD or after reperfusion. The ER stress activator thapsigargin (100 nM, Thermo Fisher Scientific, Waltham, MA, USA, Cat# T7459) and tunicamycin (50  $\mu\text{M}$ , Thermo Fisher Scientific) were added with or without neuroserpin for 4 hours before OGD and during OGD.

### Cell viability assay

Cell viability was evaluated by 3-(4,5-dimethylthiazol-2-yl)-2,5-diphenyltetrazolium bromide (Sigma-Aldrich) assay after reperfusion for 24 hours. Briefly, the medium in the 96-well plate was replaced by 30  $\mu\text{L}$  3-(4,5-dimethylthiazol-2-yl)-2,5-diphenyltetrazolium bromide (5 mg/mL) plus 70  $\mu\text{L}$  minimum essential media (Life Technologies) per well, followed by incubation for 4 hours in a  $\text{CO}_2$  incubator. The 96-well plate was centrifuged at  $159 \times g$  for 5 minutes and the 3-(4,5-dimethylthiazol-2-yl)-

2,5-diphenyltetrazolium bromide was replaced by 50  $\mu\text{L}$  dimethyl sulfoxide to dissolve the formazan crystals. The optical density value was read at 595 nm with a multimode detector (Beckman Coulter, Miami, FL, USA). Each experiment was repeated three or four times.

### Terminal deoxynucleotidyl transferase dUTP nick end labeling staining

Terminal deoxynucleotidyl transferase dUTP nick end labeling (TUNEL) staining was performed using a One Step TUNEL Apoptosis Assay Kit (Beyotime Biotechnology, Shanghai, China, Cat# C1088) following the manufacturer's instructions. Briefly, cortical neurons were fixed with 4% paraformaldehyde for 30 minutes, rinsed twice with phosphate buffered saline, and then permeabilized by 0.3% Triton X-100 for 5 minutes at room temperature. The neurons were incubated with TUNEL reaction mixture for 60 minutes at  $37^{\circ}\text{C}$  in the dark. TUNEL-positive cells were imaged under a fluorescent microscope (Axio Observer, Carl Zeiss AG, Oberkochen, Germany). Each experiment was repeated three times.

### Live and dead cell assay

Cells were labeled with a mixture of two fluorescent dyes that differentially label live and dead cells by a one-step staining procedure using a Live and Dead Cell Assay kit (Abcam, Cambridge, UK, Cat# ab115347) at 24 hours after reperfusion. Cells were washed once with Dulbecco's phosphate-buffered saline and then processed following the manufacturer's instruction. The labeled live and dead cells (green and red fluorescence, respectively) were imaged by a fluorescent microscope (Axio Observer, Carl Zeiss AG, Oberkochen, Germany) and analyzed by ImageJ (Version 1.52n, National Institutes of Health, Bethesda, MD, USA; Schneider et al., 2012). Each experiment was repeated three times.

### Western blot analysis

Ischemic brain tissues and cortical neurons were homogenized in radio immunoprecipitation assay lysis buffer (1% NP-40, 0.1% sodium dodecyl sulfate and 0.5% Na-deoxycholate in phosphate buffered saline) containing protease and phosphatase inhibitors (Selleck) and centrifuged at  $138,000 \times g$  for 15 minutes at  $4^{\circ}\text{C}$ . The supernatants were collected, and the protein concentrations were determined using a bicinchoninic acid protein assay reagent kit (Thermo Fisher Scientific) with bovine serum albumin (Thermo Fisher Scientific) as a standard. Proteins from neuronal medium were also quantified by bicinchoninic acid assay. Equal amounts of protein were separated by sodium dodecyl sulfate–polyacrylamide gel electrophoresis followed by western blot analysis following standard procedures. The blots were visualized using enhanced chemiluminescence (GE Healthcare, Chicago, IL, USA) and imaged by Amersham Imager 600 (GE Healthcare). For quantification of protein levels, the band gray value was analyzed using Quantity One software (Bio-Rad, Hercules, CA, USA), and the value of the target protein was divided by the internal reference protein to obtain the relative expression. The relative expression in the experimental group was normalized to that in the control group.

The following primary antibodies were used (with an overnight incubation at  $4^{\circ}\text{C}$ ): neuroserpin (mouse, 1:1000; Santa Cruz Biotechnology, Cat# sc-48360, RRID: AB\_628245), phosphorylated-PERK (p-PERK, rabbit, 1:1000, Cell Signaling Technology, Danvers, MA, USA, Cat# 3179S, RRID: AB\_2095853), PERK (rabbit, 1:1000, Cell Signaling Technology, Cat# 3192S, RRID: AB\_2095847), phosphorylated-eIF2 $\alpha$  (p-eIF2 $\alpha$ , rabbit, 1:1000, Cell Signaling Technology, Cat# 3398S, RRID: AB\_2096481), eIF2 $\alpha$  (rabbit, 1:1000, Cell Signaling Technology, Cat# 9722S, RRID: AB\_2230924), phosphorylated-IRE1 (p-IRE1, rabbit, 1:1000, Abcam, Cat# ab48187, RRID: AB\_873899), IRE1 (rabbit, 1:1000, Abcam, Cat# ab37037, RRID: AB\_775780), ATF6 (rabbit, 1:1000, Abcam, Cat# ab203119, RRID: AB\_2650448), ATF4 (rabbit, 1:1000; Cell Signaling Technology, Cat# 11815S, RRID: AB\_2616025), CHOP (rabbit, 1:1000, Cell Signaling Technology, Cat# 2895S, RRID: AB\_2089254), Cleaved caspase-3 (rabbit, 1:1000, Cell Signaling Technology, Cat# 9664S, RRID: AB\_2070042), glyceraldehyde-3-phosphate dehydrogenase (GAPDH, rabbit, 1:2000, Proteintech, Rosemont, IL, USA, Cat# 10494-1-AP, RRID: AB\_2263076), and  $\alpha$ -tubulin (mouse, 1:2000, Sigma-Aldrich, St. Louis, MO, USA, Cat# T8578, RRID: AB\_184122). The following secondary horseradish peroxidase-conjugated (HRP) secondary antibodies were used (with an incubation at room temperature for 1 hour): goat anti-rabbit IgG H&L (HRP) (1:2000, Cell Signaling Technology, Cat# 7074S, RRID: AB\_2099233) and goat anti-mouse IgG H&L (HRP) (1:2000, Cell Signaling Technology, Cat# 7076S, RRID: AB\_2940774). Each experiment was repeated three to six times.

### Measurement of *de novo* protein synthesis by puromycylation assay

Cells were incubated with 1  $\mu\text{M}$  puromycin (Sigma-Aldrich, Cat# 540411-100MG) for 30 minutes to label newly synthesized peptides as previously described (Liao et al., 2018; Ma et al., 2022). Cells were washed with ice-cold phosphate buffered saline and lysed in radio immunoprecipitation assay lysis buffer containing protease and phosphatase inhibitors. Puromycin-labeled peptides were analyzed by western blot using an anti-puromycin antibody (mouse, 1:10000; Millipore, Billerica, MA, USA, Cat# MABE343, RRID: AB\_2566826). *De novo* protein synthesis was determined by the total gray value of the entire lane using Quantity one software. Each experiment was repeated three times.

### Immunofluorescence staining

Cortical neurons were fixed in 4% paraformaldehyde and permeabilized with 0.4% Triton X-100. Neurons were stained with anti-MAP2 antibody (rabbit, 1:500; Millipore, Cat# AB5622, RRID: AB\_91939) overnight at 4°C, followed by incubation with Alexa Fluor 488 goat anti-rabbit (1:500; Thermo Fisher Scientific, Cat# A11034, RRID: AB\_2576217) secondary antibody. Nuclei were stained with 4',6-diamidino-2-phenylindole (1:1000, Beyotime Biotechnology, Cat# P0131-5ml) for 10 minutes. After mounting, the cells were imaged and photographed with a confocal microscope (Zeiss LSM 800, Carl Zeiss Meditec AG, Jena, Germany).

### Stereotaxic intracerebroventricular injection

Recombinant neuroserpin in artificial cerebrospinal fluid solution was administered by unilateral intracerebroventricular injection 30 minutes before MCAO procedure or immediately after reperfusion. Mice were anesthetized and placed on a stereotaxic apparatus (RWD Life Science Co., Ltd.). Next, 100 ng (2  $\mu\text{L}$ , 50 ng/ $\mu\text{L}$  in artificial cerebrospinal fluid solution) or 500 ng (1  $\mu\text{L}$ , 500 ng/ $\mu\text{L}$  in artificial cerebrospinal fluid solution) neuroserpin was injected into the right lateral ventricle (anteroposterior 0.1 mm from bregma; mediolateral 0.9 mm from the midline; dorsoventral  $-3.0$  mm from the brain surface) (Qian et al., 2022) at a rate of 0.4  $\mu\text{L}/\text{min}$  using a pulled glass capillary assembled on a stereotaxic injector with a syringe pump (Harvard Apparatus, Holliston, MA, USA). The injector was slowly withdrawn 5 minutes after injection. Artificial cerebrospinal fluid solution of equal volume (2  $\mu\text{L}$  for the control of 100 ng neuroserpin, and 1  $\mu\text{L}$  for the control of 500 ng neuroserpin) was injected as the vehicle control. For ER stress induction, tunicamycin was dissolved in normal saline (0.05 mg/mL) and intraperitoneally administered to mice (0.5 mg/kg, i.e., 10  $\mu\text{L}/\text{g}$  body weight) 2 days before MCAO (Wu et al., 2018). An equal volume of saline (10  $\mu\text{L}/\text{g}$  body weight) was intraperitoneally administered as the vehicle control.

### RNA sequencing

Cortices of the ischemic hemisphere were collected for RNA sequencing (RNA-seq) 24 hours after MCAO. Briefly, total RNA was extracted using Trizol reagent (Invitrogen, Waltham, MA, USA, Cat# 15596026). RNA purity and quantification were evaluated using Qubit4.0 (Thermo Fisher Scientific), and RNA integrity was assessed using an Agilent 2100 Bioanalyzer (Agilent Technologies, Santa Clara, CA, USA). The libraries were constructed using the HiSeq NGS® Ultima Dual-mode mRNA Library Prep Kit for Illumina® (Yeast Biotechnology (Shanghai) Co., Ltd., Shanghai, China). RNA-seq was performed on the DNBSEQ-T7 platform (Geneplus-Shenzhen, Shenzhen, China). FastQC (v0.12.1) and MultiQC (v1.14; <https://github.com/s-andrews/FastQC/>) were used for raw data quality control. Sequencing data were mapped to the mouse reference genome (GRCm39, NCBI Annotation Release 109; [https://www.ncbi.nlm.nih.gov/datasets/genome/GCF\\_000001635.27/](https://www.ncbi.nlm.nih.gov/datasets/genome/GCF_000001635.27/)) and quantified to raw read counts using STAR (v2.7.10a; <https://github.com/alexdobin/STAR/>) (Dobin et al., 2013). Raw read counts were filtered under the standard that read counts are no less than 1 in all samples; only protein coding genes were considered for further analysis. Differentially expressed genes (DEGs) were identified by  $|\log_2(\text{fold change})| \geq 1$  and adjusted  $P$  value  $< 0.05$  using DESeq2 package (v1.38.3; <https://www.bioconductor.org/packages/release/bioc/html/DESeq2.html>) (Wu et al., 2021). Gene Ontology (GO) enrichment and Gene Set Enrichment Analysis were conducted using cluster Profiler package (v4.9.0; <https://github.com/YuLab-SMU/clusterProfiler>) (Love et al., 2014). Gene expression was normalized to transcript per million mapped to generate principal component analysis plot and volcano plots.

### Statistical analysis

Although no statistical methods were used to predetermine sample sizes for *in vivo* studies, the sample sizes were comparable to those reported in

previous publications (Chen et al., 2023a; Liu et al., 2023). If any animal died, it was excluded from subsequent analysis. Data were collected by a blinded evaluator. Data are presented as mean  $\pm$  standard error of mean (SEM) from at least three independent experiments. Statistical analysis was performed using GraphPad Prism 9.0.0 software (GraphPad Software, San Diego, CA, USA, [www.graphpad.com](http://www.graphpad.com)). Comparisons between two groups and multiple groups were evaluated by unpaired  $t$ -test and one-way analysis of variance followed by the Dunnett's multiple comparison test, respectively. The specific analysis used for each evaluation is stated in the figure legends. Neurological scores (discrete values) were analyzed using Mann-Whitney  $U$  test or Kruskal-Wallis test, followed by Dunnett's multiple comparison test.  $P < 0.05$  indicates statistical significance.

## Results

### Cerebral ischemia-reperfusion injury induces early activation of endoplasmic reticulum transmembrane stress sensors and late activation of endoplasmic reticulum-mediated apoptosis

To investigate the temporal profile of ER stress in cerebral I/R injury, cerebral ischemia was induced in adult mice by MCAO for 1.5 hours, and samples were collected at different time points (ranging from 0 to 24 hours) after reperfusion (Figure 1A). The effectiveness of MCAO was confirmed by detection of cerebral infarction, compromised neurological function including motor and sensory dysfunction, and loss of reflexes and balance by Zea-Longa test after 24 hours of reperfusion (Figure 1B–D). The ischemic brain tissues were collected after 1.5 hours of MCAO (reperfusion 0 hours) or 1, 3, 6, 12, and 24 hours after reperfusion to monitor the time-dependent expression/activity changes of the ER stress signaling molecules eIF2 $\alpha$ , IRE1, ATF6, ATF4, and CHOP (Figure 1E). Tissues from the sham group were collected at 1.5 hours after the sham surgery. eIF2 $\alpha$  phosphorylation, IRE1 phosphorylation, and ATF6 expression all exhibited a sharp increase immediately after cerebral ischemia and were sustained during the first 1, 3, and 6 hours of reperfusion, respectively, followed by a decrease to normal levels after 12 hours (Figure 1F–H). Notably, ATF4 and CHOP, the key pro-apoptotic transcription factors linking ER stress to apoptosis (Liu and Ju, 2024), were activated at later time points of reperfusion (Figure 1I and J). These findings revealed that cerebral I/R injury induces a rapid and transient activation of ER stress protein sensors followed by upregulation of apoptosis.

### Oxygen-glucose deprivation reperfusion induces transient activation of endoplasmic reticulum stress sensors followed by subsequent apoptosis, which is ameliorated by endoplasmic reticulum stress inhibitors

We then further investigated the role of ER stress in I/R injury using the OGD/R-damaged primary cortical neuron *in vitro* model. The purity of primary cultured cortical neurons was confirmed to be  $\sim 90\%$ , quantified by the percentage of cells with immunoreactivity of MAP2, a marker of neuronal dendrites (Additional Figure 1). As previously established (Shi et al., 2019), 4 hours of OGD followed by 24 hours of reperfusion in 7 DIV cortical neurons led to a 40% decrease in cell viability (Figure 2A and B). Cell lysates were harvested at various time points of OGD and reperfusion, and different ER stress signaling molecules were examined (Figure 2C). Consistent with the observations in the MCAO mice, OGD induced strong activation of all ER transmembrane stress sensors, including PERK (and its substrate eIF2 $\alpha$ ), IRE1, and ATF6. The phosphorylation of PERK, eIF2 $\alpha$ , and IRE1 and the expression of ATF6 all peaked at the beginning of reperfusion and then gradually decreased to normal levels after 1–4 hours (Figure 2D–G).

As ER stress leads to inhibited mRNA translation (Chen et al., 2023b), we also investigated the temporal changes of *de novo* protein synthesis using the puromycylation assay. OGD remarkably suppressed global protein synthesis, which gradually recovered to normal level after 2 hours of reperfusion (Figure 2H), coinciding with the change pattern of ER stress sensors. By contrast, apoptosis signaling molecules were activated at later stages of reperfusion; ATF4 and CHOP increased at 12 hours of reperfusion, and cleaved caspase-3 peaked at 24 hours of reperfusion (Figure 2I–K). Taken together, our experiments showed that ER stress activation and protein synthesis inhibition occurred at the end of OGD and they gradually recovered during the early phase of reperfusion, whereas apoptosis activation occurred later. Notably, the ER stress activator thapsigargin, which induces the ER stress response by non-competitive inhibition of the ER Ca<sup>2+</sup> ATPase, induced a similar signaling transduction sequence to that induced by OGD/R in cultured cortical neurons, suggesting that OGD/R-induced signaling changes are largely mediated by ER stress conditions (Additional Figure 2).

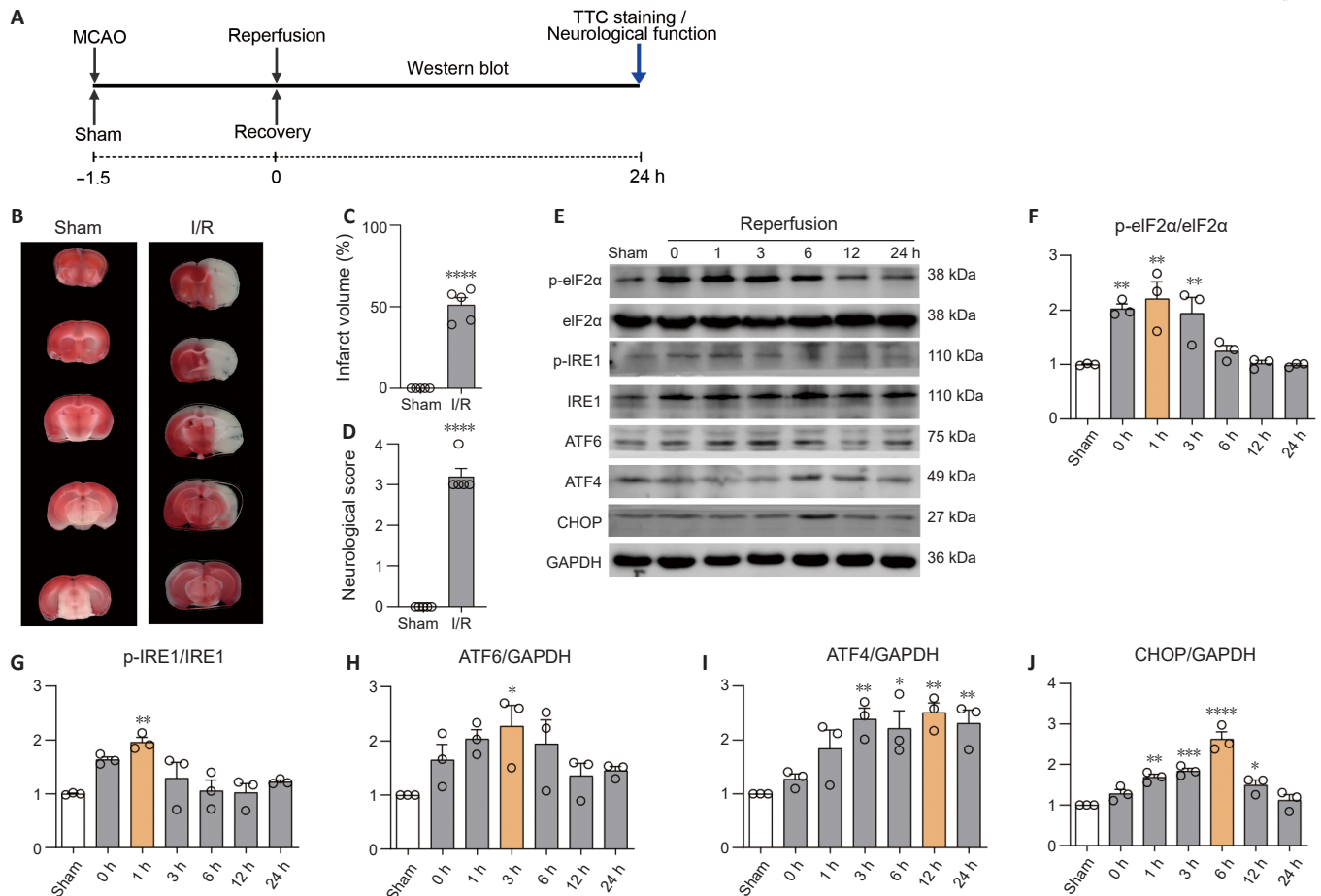


**Figure 1 | Cerebral I/R induces transient activation of ER stress transmembrane sensors, followed by apoptosis.**

(A) Schematic representation of the timeline of the experimental procedure. Mice were subjected to sham/MCAO for 1.5 hours followed by recovery/reperfusion. Brain tissues were collected at various time points during reperfusion for Western blotting, and brain infarction and neurological evaluation were performed after 24 hours recovery/reperfusion. (B) Triphenyl-tetrazolium chloride-stained cerebral coronal sections from representative brains, collected at 24 hours after reperfusion. The infarcted area is shown in white, and the normal area is shown in red. (C) Statistical analysis of the infarct volumes ( $n = 5$ ). \*\*\*\* $P < 0.0001$ , I/R group vs. sham group, unpaired  $t$ -test. (D) Statistical analysis of the neurological scores 24 hours after reperfusion by Zea-Longa test ( $n = 5$ ). \*\*\*\* $P < 0.0001$ , I/R group vs. sham group, Mann-Whitney  $U$  test. (E–J) The ischemic brain tissues were collected after 1.5 hours of MCAO (reperfusion 0 hours) or 1, 3, 6, 12, and 24 hours after reperfusion. The tissues from the sham group were collected at 1.5 hours after the sham surgery. (E) Representative western blot images of p-eIF2 $\alpha$ , eIF2 $\alpha$ , p-IRE1, ATF6, ATF4, and CHOP at different time points ( $n = 3$ ) after reperfusion. (F–J) Quantifications of the normalized levels of p-eIF2 $\alpha$ /eIF2 $\alpha$  (F), p-IRE1/IRE1 (G), ATF6/GAPDH (H), ATF4/GAPDH (I), and CHOP/GAPDH (J). \* $P < 0.05$ , \*\* $P < 0.01$ , \*\*\* $P < 0.001$ , \*\*\*\* $P < 0.0001$ , I/R group vs. sham group, one-way analysis of variance followed by Dunnett’s multiple comparison test. Data are shown as mean  $\pm$  SEM. ATF: Activating transcription factor; CHOP: CCAAT/enhancer binding protein homologous protein; eIF2 $\alpha$ : eukaryotic translation initiation factor 2 $\alpha$ ; ER: endoplasmic reticulum; GAPDH: glyceraldehyde-3-phosphate dehydrogenase; I/R: cerebral ischemia-reperfusion; IRE1: inositol requiring enzyme 1; MCAO: middle cerebral artery occlusion; p-: phosphorylated; TTC: 2,3,5-triphenyl tetrazolium chloride.

To investigate whether early ER stress leads to the late phase of cell injury, 4-PBA or salubrinal at dosages that do not influence cell viability were used to inhibit ER stress (Additional Figure 3; Boyce et al., 2005; Gao et al., 2013; Sharma et al., 2016). 4-PBA is a potent chemical chaperone that alleviates the unfolded protein response and acts as an ER stress inhibitor (Sharma et al., 2016). Salubrinal is a selective inhibitor of eIF2 $\alpha$  dephosphorylation independent of the eIF2 $\alpha$  kinase PERK, offering protection against ER stress-induced apoptosis; it has been used as an inhibitor of ER stress in several studies (Boyce et al., 2005; Sokka et al., 2007; Gong et al., 2012; Gao et al., 2013; Kim et al., 2014). Either 4-PBA or salubrinal was added to cortical neurons at 1 hour before OGD and maintained during OGD, but not during reperfusion (Figure 2L). Both inhibitors substantially alleviated the cell damage caused by OGD/R (Figure 2M and N), suggesting that early-stage inhibition of ER stress effectively protects neurons against OGD/R injury.

**Neuroserpin secretion is inhibited by oxygen-glucose deprivation, and the addition of extracellular neuroserpin protects neurons against oxygen-glucose deprivation reperfusion damage**

Neuroserpin is produced by several types of neurons and is a secretory protein with neuroprotective effects. We thus examined whether OGD influences the intracellular or secreted levels of neuroserpin in cortical neurons. Notably, neuroserpin level was not altered in the cell homogenate containing intracellular and membrane proteins, but cellular neuroserpin

mRNA and extracellular neuroserpin protein were both markedly decreased by OGD (Figure 3A–D), suggesting substantial inhibition of gene expression and extracellular protein secretion of neuroserpin. Consistent with the *in vitro* results, the mRNA level of neuroserpin was also markedly downregulated in brain tissues of MCAO mice (Figure 3E). We speculated that the deprivation of secreted neuroserpin leads to weakened neuroprotection, thereby contributing to OGD/R-induced cellular damage. To test this hypothesis, we collected the conditioned medium from normal cortical neurons cultured in standard conditions. Instead of adding new culture medium to OGD-injured neurons, we added the conditioned medium containing secreted neuroserpin for the reperfusion phase (Figure 3F). Conditioned medium treatment markedly increased the cell viability of OGD/R-injured neurons. Moreover, when anti-neuroserpin antibody was used to neutralize neuroserpin in the conditioned medium, the protective effect of the conditioned medium was canceled (Figure 3G). These results suggest that secreted neuroserpin is an important factor for neuroprotection, and OGD substantially inhibits its secretion from the endogenous sources, thus worsening cell survival.

Our results showed that extracellular neuroserpin alleviates cell damage. We thus next examined whether the addition of recombinant neuroserpin also has a protective effect. Neuroserpin (1–20 ng/mL) was pretreated to 7 DIV cortical neurons for 4 hours and was continuously present during the 4 hours of OGD phase but was absent during the reperfusion phase (Figure 3H). Neuroserpin effectively alleviated OGD/R-induced damage at 20 ng/mL

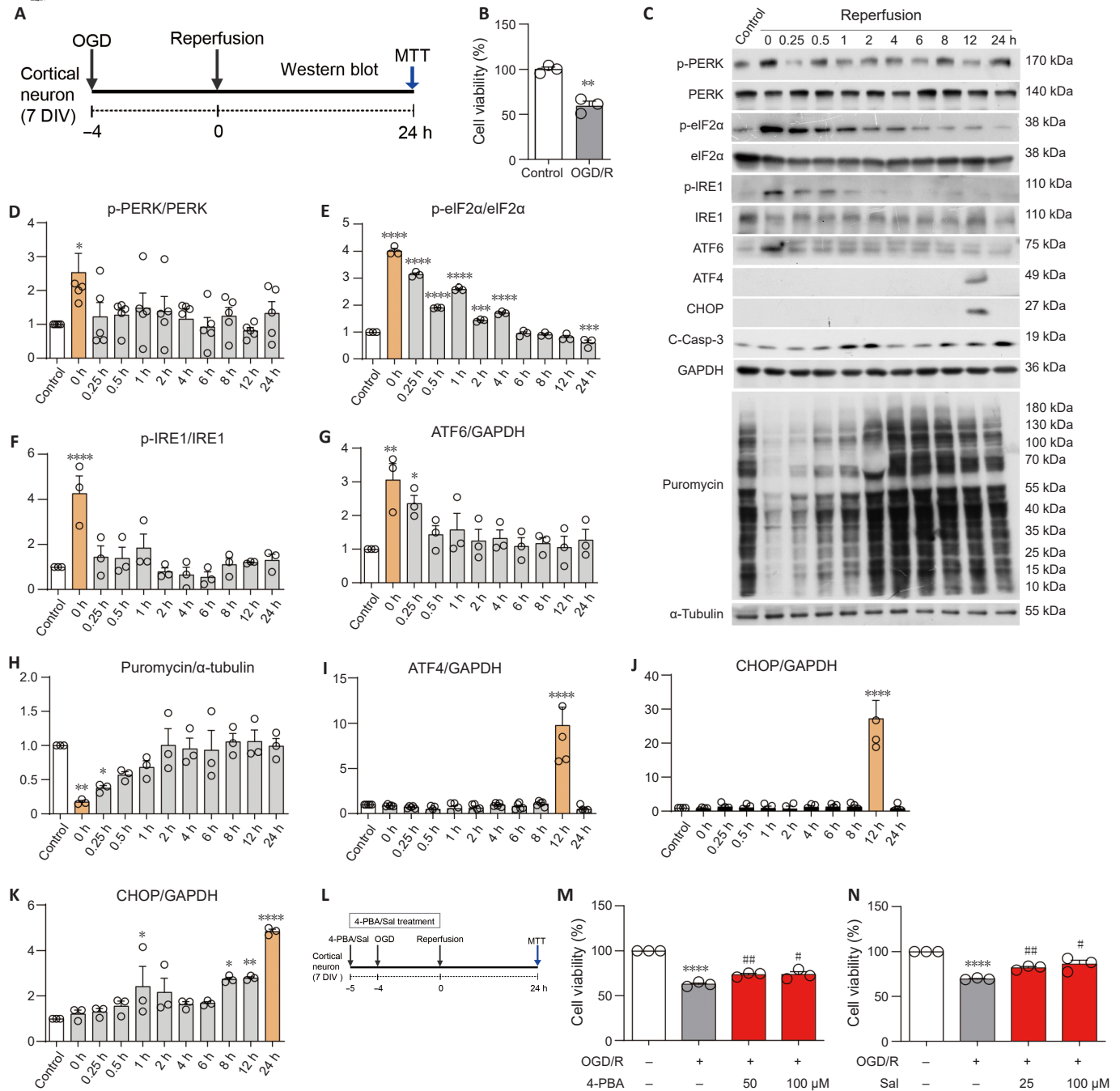


**Figure 2 | OGD/R induces early activation of ER stress sensors followed by apoptosis in cultured cortical neurons, which is ameliorated by ER stress inhibitors.**

(A) Schematic representation of the timeline of the experimental procedures. Cortical neurons (7 DIV) were cultured in normal conditions (Control group) or exposed to oxygen/glucose deprivation for 4 hours followed by reperfusion (OGD/R group). Cell lysates were collected at various time points for Western blotting, and cell viability was evaluated after 24 hours reperfusion. (B) The cell viability of primary cortical neurons after OGD/R 24 hours was detected by MTT assay. Cortical neurons (7 DIV) under standard culture conditions were used as the control group ( $n = 3$ ).  $**P < 0.01$ , vs. control, unpaired  $t$ -test. (C) Cell lysates from the OGD/R group were collected at different time points (0–24 hours) after reperfusion. For the control group, cell lysates were collected at the same time corresponding to 0 hours reperfusion of OGD/R group. Levels of ER stress sensors, protein synthesis, and apoptosis-related proteins were examined by western blot analysis. (D–K) Quantifications of the normalized levels of p-PERK/PERK (D,  $n = 4$ ), p-eIF2 $\alpha$ /eIF2 $\alpha$  (E,  $n = 3$ ), p-IRE1/IRE1 (F,  $n = 3$ ), ATF6 (G,  $n = 3$ ), puromycin (H,  $n = 3$ ), ATF4 (I,  $n = 3$ ), CHOP (J,  $n = 3$ ), and cleaved-caspase-3 (K,  $n = 3$ ). GAPDH and  $\alpha$ -tubulin served as the loading control.  $*P < 0.05$ ,  $**P < 0.01$ ,  $***P < 0.001$ ,  $****P < 0.0001$ , vs. control, one-way analysis of variance followed by Dunnett's multiple comparison test. (L) A schematic illustration of the application of ER stress inhibitors, sodium 4-PBA or Sal, to neurons 1 hour before OGD and during OGD (–5 to 0 hours). (M, N) MTT assay was performed to evaluate cell viability of neurons treated with 4-PBA or Sal ( $n = 3$ ).  $****P < 0.0001$ , OGD/R vs. control;  $\#P < 0.05$ ,  $\#\#P < 0.01$ , 4-PBA (50 or 100  $\mu$ M) or Sal (25 or 100  $\mu$ M) vs. OGD/R, unpaired  $t$ -test. Data are shown as mean  $\pm$  SEM. 4-PBA: Sodium 4-phenylbutyrate; ATF: activating transcription factor; CHOP: CCAAT/enhancer binding protein homologous protein; C-Casp-3: cleaved-caspase-3; DIV: day *in vitro*; eIF2 $\alpha$ : eukaryotic translation initiation factor 2 $\alpha$ ; ER: endoplasmic reticulum; GAPDH: glyceraldehyde-3-phosphate dehydrogenase; IRE1: inositol requiring enzyme 1; MTT: 3-(4,5-Dimethyl-2-thiazolyl)-2,5-diphenyl-2H-tetrazolium bromide; OGD: oxygen-glucose deprivation; OGD/R: oxygen-glucose deprivation/reperfusion; p-: phosphorylated-; PERK: double-stranded RNA-activated protein kinase-like ER kinase; Sal: salubrinal.

(Figure 3I). We further used the live and dead cell assay to visualize cell viability. OGD/R triggered a pronounced decreased number of viable cells and an increased number of damaged cells, but the addition of neuroserpin prevented OGD-induced cell damage (Figure 3J and K). We further examined whether neuroserpin could reverse cell damage when applied after OGD (Figure 3L). Neuroserpin (50 and 100 ng/mL) markedly enhanced cell viability

of the OGD/R-injured cells (Figure 3M). Consistent with the cell viability results, the numbers of TUNEL-positive apoptotic cells markedly increased after OGD/R, whereas neuroserpin (20 and 100 ng/mL) reversed the apoptosis level (Figure 3N and O). These results showed that complementing endogenous extracellular neuroserpin by adding exogenous protein improves cell survival against OGD/R.

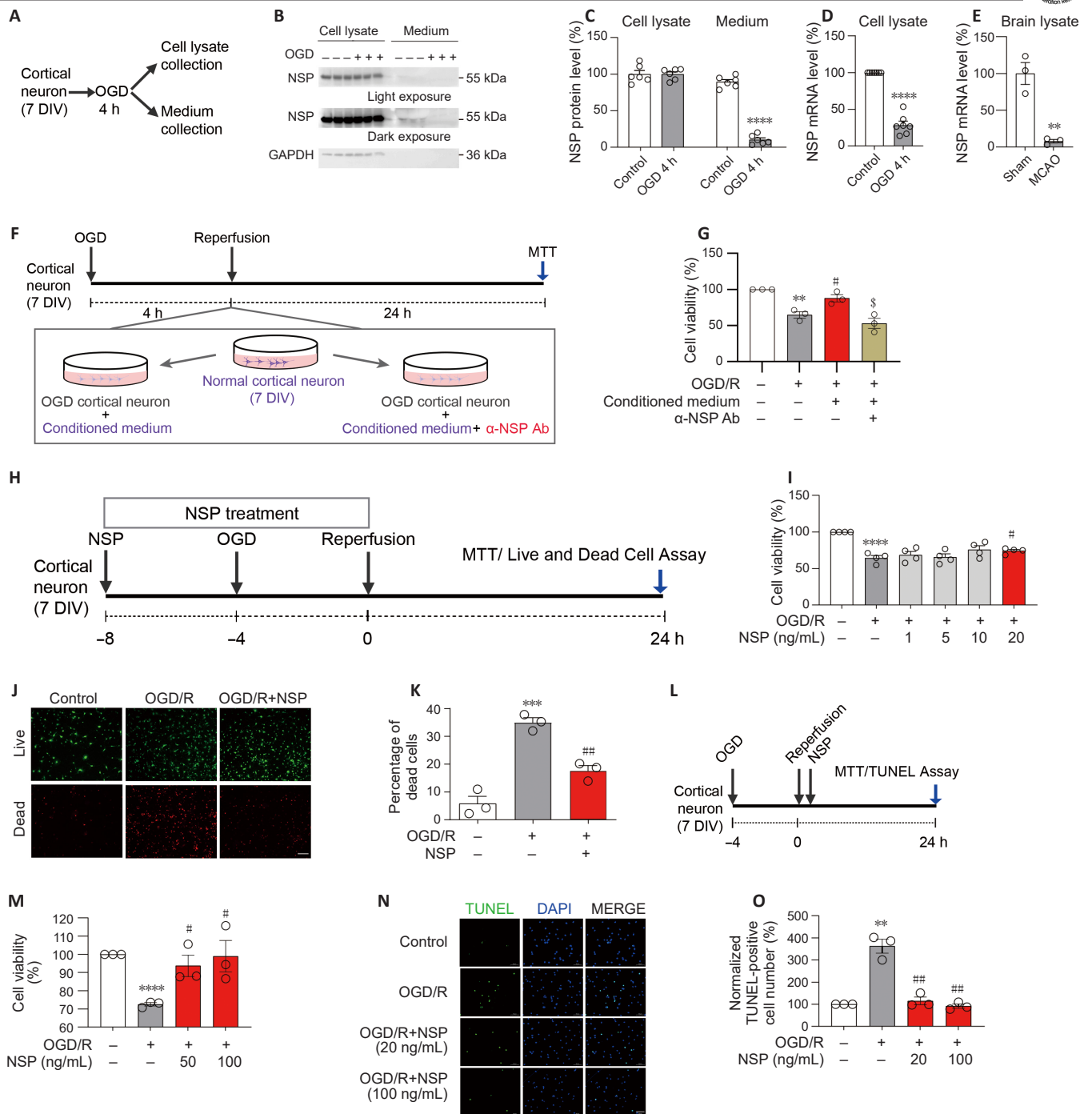


**Figure 3 | Secreted neuroserpin ameliorates cell death in cultured cortical neurons.**

(A) Schematic of the experiment: cell lysates and media of cortical neurons (7 DIV) were collected separately and analyzed individually for NSP levels after 4 hours of OGD. (B) Representative western blot images showing the cellular and secreted levels of NSP. (C) Quantifications of NSP protein levels in cell lysate or medium from primary cortical neurons after 4 hours of OGD by Western blot assay ( $n = 6$ ).  $****P < 0.0001$ , OGD 4 h vs. control, unpaired  $t$ -test. (D) Quantifications of the cellular NSP mRNA level in cell lysate from primary cortical neurons after 4 hours of OGD by quantitative polymerase chain reaction ( $n = 7$ ).  $****P < 0.0001$ , OGD 4 h vs. control, unpaired  $t$ -test. (E) Neuroserpin mRNA levels in brain tissues of sham and MCAO mice by quantitative polymerase chain reaction ( $n = 3$  mice per group).  $**P < 0.01$ , control vs. MCAO, unpaired  $t$ -test. (F) A diagram showing the conditional medium treatment procedure. Conditioned medium was collected from normal neurons of the same stage (7 DIV) and added to OGD-injured neurons for the reperfusion phase. To neutralize NSP in the medium, anti-NSP antibody ( $\alpha$ -NSP Ab; 50 ng for 20,000 cells) was added in the conditional medium. (G) Cell viability was measured by MTT assay in OGD/R neurons cultured in conditioned medium with or without  $\alpha$ -NSP Ab ( $n = 3$ ).  $**P < 0.01$ , OGD/R vs. control;  $\#P < 0.05$ , OGD/R + conditioned medium vs. OGD/R;  $\$P < 0.05$ , OGD/R + conditioned medium +  $\alpha$ -NSP Ab vs. OGD/R + conditioned medium, unpaired  $t$ -test. (H) A diagram showing the recombinant NSP treatment procedure. NSP (1–20 ng/mL) was added to neurons 4 hours before OGD and during OGD and after reperfusion. (I) Cell viability of neurons treated with different concentrations of NSP was determined by MTT assay ( $n = 4$ ).  $****P < 0.0001$ , OGD/R vs. control;  $\#P < 0.05$ , OGD/R + NSP vs. OGD/R, unpaired  $t$ -test. (J) Representative images of live and dead neurons, treated with 20 ng/mL NSP, measured by the live and death cell assay. Scale bar: 200  $\mu$ m. (K) Quantification of the percentage of dead cells ( $n = 3$ ).  $***P < 0.001$ , OGD/R vs. control;  $\#\#\#P < 0.01$ , OGD/R + NSP vs. OGD/R, unpaired  $t$ -test. (L) A diagram showing the experimental procedure: NSP (50 and 100 ng/mL) was added to neurons immediately after OGD. (M) Cell viability of neurons treated with different concentrations of NSP were determined by MTT assay ( $n = 3$ ).  $****P < 0.0001$ , OGD/R vs. control;  $\#P < 0.05$ , OGD/R + NSP vs. OGD/R, unpaired  $t$ -test. (N) Representative TUNEL and DAPI staining in OGD/R-injured neurons treated with NSP (20 and 100 ng/mL). Scale bar: 100  $\mu$ m. (O) Number of TUNEL-positive cells in each group was quantified and normalized to that of the control group ( $n = 3$ ).  $**P < 0.01$ , OGD/R vs. control;  $\#\#\#P < 0.01$ , OGD/R + NSP vs. OGD/R, unpaired  $t$ -test. Data are shown as mean  $\pm$  SEM.  $\alpha$ -NSP Ab: Anti-NSP antibody; DAPI: 4',6-diamidino-2-phenylindole; DIV: day *in vitro*; GAPDH: glyceraldehyde-3-phosphate dehydrogenase; MCAO: middle cerebral artery occlusion; MTT: 3-(4,5-dimethyl-2-thiazolyl)-2,5-diphenyl-2H-tetrazolium bromide; NSP: neuroserpin; OGD: oxygen-glucose deprivation; OGD/R: oxygen-glucose deprivation/reperfusion; TUNEL: terminal deoxynucleotidyl transferase dUTP nick end labeling.

### Neuroserpin inhibits oxygen-glucose deprivation reperfusion-induced endoplasmic reticulum stress and subsequent apoptosis signaling pathways

As the presence of neuroserpin at an early stage protects neurons from OGD/R injury, we investigated whether this effect occurs via the inhibition of ER stress. We added neuroserpin (or vehicle) before and during OGD, and the cell lysates were collected at different time points for the detection of the maximum activation/deactivation levels of different signaling events. All ER stress molecules and *de novo* protein synthesis were analyzed immediately after OGD, ATF4 and CHOP were analyzed at 12 hours, and cleaved caspase-3 at 24 hours of reperfusion (Figure 4A). Neuroserpin treatment substantially reversed all the above signaling changes induced by OGD/R (Figure 4B and C). The immediate increase of ER stress sensors p-PERK, p-IRE1, ATF6, and p-eIF2 $\alpha$  and the inhibition of global protein synthesis after OGD was suppressed by neuroserpin (Figure 4D–H). The subsequent activation of apoptosis molecules ATF4, CHOP, and cleaved caspase-3 was also effectively inhibited by neuroserpin (Figure 4I–K). Application of neuroserpin in normoxic neurons did not show any obvious effect on the expression of these molecules (Figure 4D–K). Therefore, supplementing neuroserpin at the OGD phase effectively inhibits the early stage of ER stress activation and greatly prevents the subsequent programmed apoptosis at the later stage of reperfusion.

### Neuroserpin alleviates oxygen-glucose deprivation reperfusion-induced neuronal damage *in vitro* and cerebral ischemia-reperfusion injury *in vivo* through inhibition of endoplasmic reticulum stress

To verify whether the protective effects of neuroserpin against I/R were achieved through inhibiting ER stress, we elevated the ER stress levels at the beginning of OGD by pretreatment with thapsigargin (100 nM) or another ER stress activator tunicamycin (50  $\mu$ M), which induces ER stress response by inhibiting protein glycosylation (Figure 5A). These two ER stress activators alone did not aggravate cell damage by OGD/R (Figure 5B and C). However, pretreatment of either thapsigargin or tunicamycin abrogated the effects of neuroserpin (20, 50, or 100 ng/mL) on improving cell survival (Figure 5B, C, and Additional Figure 4). These results suggest that ER stress inhibition at an early stage mediates the neuroprotection of neuroserpin. Next, we examined whether the neuroprotective effect of neuroserpin is blocked by ER stress activation *in vivo*. Multiple studies have shown that neuroserpin protects against cerebral I/R damage (Yepes et al., 2000; Cinelli et al., 2001; Zhang et al., 2002; Cai et al., 2020; Ding et al., 2021). We delivered recombinant neuroserpin (100 ng) into the brain of mice by intracerebroventricular administration 30 minutes before MCAO surgery (Figure 5D). Consistent with published observations (Zhang et al., 2002; Cai et al., 2020), neuroserpin substantially reduced infarct volume and improved neurological function (Figure 5E–G). To enhance ER stress at the initial stage of MCAO, tunicamycin (0.5 mg/kg) was intraperitoneally injected 2 days before neuroserpin administration to mildly elevate brain ER stress (Figure 5D; Wu et al., 2018). Notably, although tunicamycin alone did not worsen the cerebral I/R injury, it blocked the effect of neuroserpin on reducing the infarct volume and improving neurological function (Figure 5E–G). To assess whether neuroserpin treatment after brain ischemia also has a protective effect via inhibition of ER stress, tunicamycin or vehicle was intraperitoneally injected 2 days before MCAO, and recombinant neuroserpin (500 ng) was intracerebroventricularly administered immediately after ischemia (Figure 5H). Indeed, acute application of neuroserpin after ischemia remarkably lowered the infarct volume and neurological score, and these effects were blocked by tunicamycin (Figure 5I–K). Taken together, these findings showed that neuroserpin reduces I/R injury both *in vitro* and *in vivo*, which is mainly dependent on inhibition of the ER stress response.

### Transcriptomic analysis reveals that neuroserpin rescues endoplasmic reticulum stress and neuronal apoptosis in middle cerebral artery occlusion mice

To further investigate the potential molecular mechanisms of neuroserpin in cerebral ischemia, total RNA was isolated from the cortices of the ischemic hemisphere at 24 hours after MCAO and subjected to transcriptomic analysis. Principal component analysis on RNA-seq data showed that the transcriptome of the MCAO group differed dramatically from the sham group, whereas neuroserpin administration data were clustered between these two groups, suggesting that neuroserpin administration partially reversed the transcriptome variation caused by MCAO (Figure 6A). In total, 2374 DEGs (defined as  $|\log_2(\text{fold change})| \geq 1$  and adjusted *P* value < 0.05) were identified in the MCAO group compared with the sham group, which included

1794 upregulated DEGs (75.6% of the total DEGs) and 580 downregulated DEGs (24.4% of the total DEGs). There were 1151 DEGs identified in the neuroserpin group compared with the MCAO group, including 1027 downregulated DEGs (89.3% of total DEGs) and 124 upregulated DEGs (10.7% of total DEGs) (Figure 6B and C). Overall, there were more upregulated than downregulated genes in the MCAO group compared with the sham group, whereas most of the DEGs were downregulated in the neuroserpin group compared with the MCAO group, suggesting that neuroserpin has an opposite effect on the overall transcriptional change caused by MCAO.

We then performed GO analysis to understand the functional enrichment of DEGs. The upregulated DEGs in the MCAO group were mainly enriched in processes related to ER stress and neuron apoptotic process, such as regulation of neuron death, neuron apoptotic process, response to ER stress, cellular response to unfold protein, ER unfolded protein response, and regulation of chemokine. The downregulated DEGs in the MCAO group were enriched in synapse, such as regulation of postsynaptic membrane potential, synapse assembly, postsynapse organization, potassium ion transport, and regulation of synapse structure or activity (Figure 6D). Conversely, in the neuroserpin group, the upregulated DEGs were mainly enriched in processes related to synapse, such as regulation of membrane potential, gated channel activity, potassium ion transport, postsynaptic membrane, neurotransmitter receptor activity, and GABAergic synapse; the downregulated DEGs were enriched in ER stress and neuron apoptosis, such as leukocyte apoptotic process, regulation of neuron death, ER lumen, response to unfolded protein, and regulation of chemokine production (Figure 6E).

To further characterize the transcriptomic changes related to ER stress and synaptic function in each comparison, we used Gene Set Enrichment Analysis to identify statistically enriched gene sets in the transcriptomic data (Figure 6F). ER stress-related processes were markedly upregulated in the MCAO group, including response to ER stress and response to unfolded protein, along with other related processes such as neuron apoptotic process and regulation of immune response. Furthermore, synaptic function-related processes were markedly downregulated in the MCAO group, including GABAergic synapse, regulation of postsynaptic membrane potential, chemical synaptic transmission, and neurotransmitter secretion. The above processes were correspondingly reversed in the neuroserpin group (Figure 6F). By comparing the MCAO vs. sham DEG list with the neuroserpin vs. MCAO DEG list, we found that 908 out of 1794 (~50.7%) of the upregulated MCAO vs. sham DEGs were reversely downregulated by neuroserpin (Figure 6G). Furthermore, these genes were enriched in GO biological processes related to neuronal apoptosis and ER stress (Figure 6H). Additionally, 71 out of 580 (~12.2%) of the downregulated MCAO vs. sham DEGs were reversed as upregulated neuroserpin vs. MCAO DEGs (Figure 6I). These genes were enriched in GO sets related to ion transport and synapse (Figure 6J). Taken together, these data reveal that the administration of neuroserpin markedly alters the transcriptome of MCAO mice, resulting in the expression of a substantial number of genes, particularly those associated with ER stress, apoptosis, and synapse function.

## Discussion

ER stress plays critical roles in the complex pathophysiology that underlies cerebral I/R. Strong evidence indicates that the inhibition of ER stress can effectively mitigate experimental cerebral I/R injury, and therefore ER stress is a potential therapeutic target for ischemic stroke (Xin et al., 2014; Thiebaut et al., 2019; Han et al., 2021b; Wang et al., 2022). ER stress is detrimental to neuronal survival as it leads to dysregulated proteostasis and cell death; however, ER stress also mediates adaptation for cell survival when unfolded proteins accumulate during cell damage (Luchetti et al., 2023; Li et al., 2024). Therefore, ER stress-targeted intervention strategies should be used with caution. Importantly, the time sequence and causal relations of ER stress signaling transduction in I/R and the ER stress-targeted therapeutic time window have not been fully established. Using *in vitro* and *in vivo* models, we demonstrated that ER stress was rapidly activated with concomitant inhibition of protein synthesis by ischemia/OGD. With prolonged reperfusion time, ER stress and protein synthesis recovered, but apoptosis gradually increased. We also showed that inhibition of the rapid activation of ER stress during the early stage of reperfusion effectively reduced neuronal apoptosis during the late stage of reperfusion. Inhibiting ER stress before or after ischemia was found to reduce the damage caused by I/R (Lv et al., 2023). Moreover, neuroserpin increased the time window of

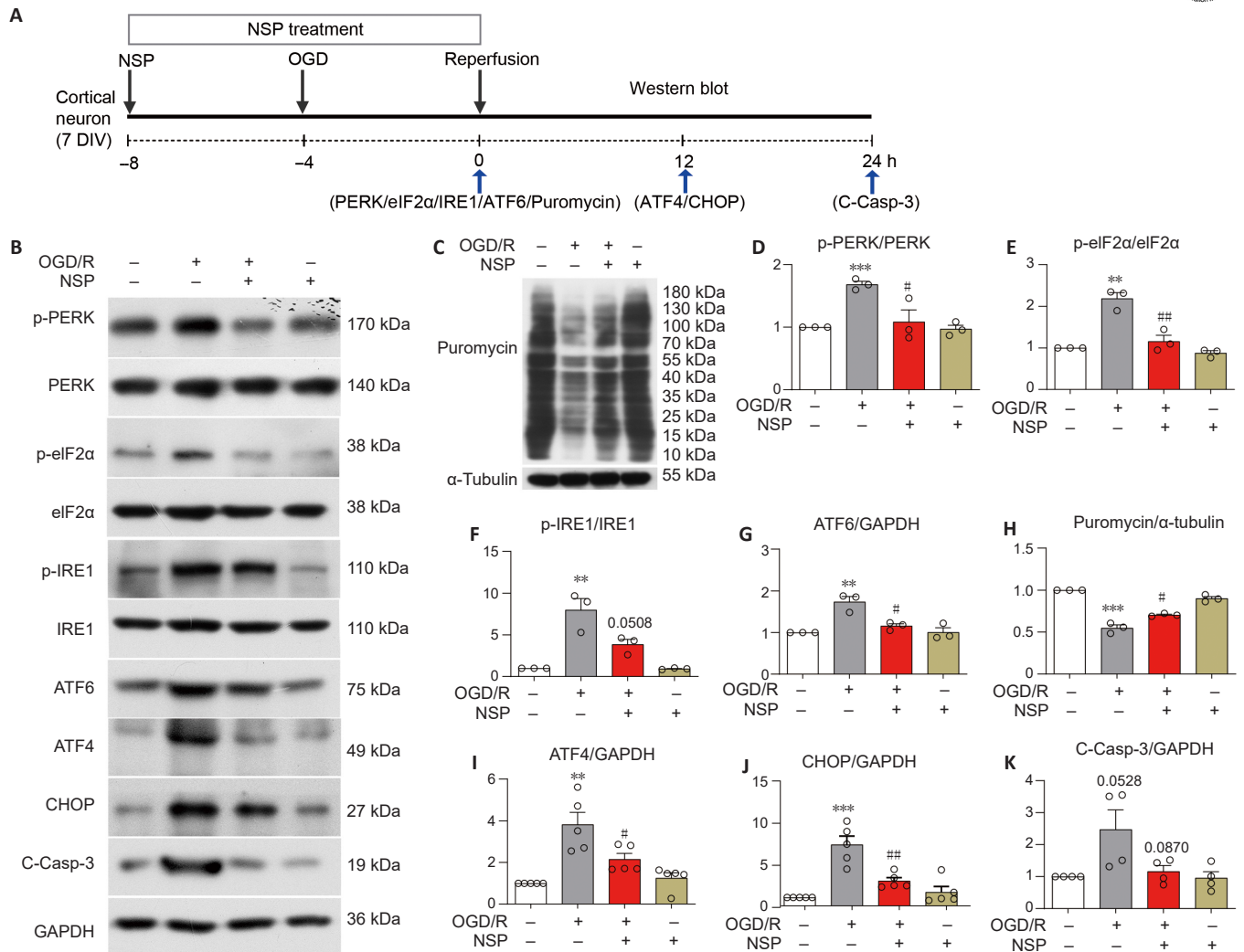


**Figure 4 | Neuroserpin inhibits ER stress-mediated signaling transduction induced by OGD/R.**

(A) Schematic representation of the timing of the experimental procedures. Neuroserpin (NSP; 20 ng/mL) was added to cortical neurons (7 DIV) 4 hours before OGD and during OGD, followed by reperfusion. Cell lysates were collected at the indicated time points of reperfusion for the examination of ER stress signaling molecules. (B) Representative western blots showing phosphorylated and total levels of ER stress sensors and apoptosis-related proteins. (C) Representative western blots showing levels of puromycin. (D–K) Quantitative analysis of the normalized p-PERK/PERK (D,  $n = 3$ ), p-eIF2 $\alpha$ /eIF2 $\alpha$  (E,  $n = 3$ ), p-IRE1/IRE1 (F,  $n = 3$ ), ATF6 (G,  $n = 3$ ), puromycin (H,  $n = 3$ ), ATF4 (I,  $n = 5$ ), CHOP (J,  $n = 5$ ), and cleaved-caspase-3 (K,  $n = 4$ ). GAPDH and  $\alpha$ -tubulin were used as loading controls. \*\* $P < 0.01$ , \*\*\* $P < 0.001$ , OGD/R vs. control; # $P < 0.05$ , ## $P < 0.01$ , OGD/R + NSP vs. OGD/R, unpaired  $t$ -test. Data are shown as mean  $\pm$  SEM. ATF: Activating transcription factor; CHOP: CCAAT/enhancer binding protein homologous protein; C-Casp-3: cleaved-caspase-3; DIV: day *in vitro*; eIF2 $\alpha$ : eukaryotic translation initiation factor 2 $\alpha$ ; ER: endoplasmic reticulum; GAPDH: glyceraldehyde-3-phosphate dehydrogenase; IRE1: inositol requiring enzyme 1; i.c.v.: intracerebroventricular; NSP: neuroserpin; OGD: oxygen-glucose deprivation; OGD/R: oxygen-glucose deprivation/reperfusion; p-: phosphorylated-; PERK: double-stranded RNA-activated protein kinase-like ER kinase.

thrombolysis treatment via tissue-type fibrinogen activator in stroke in rats (Zhang et al., 2002). Therefore, ER stress suppression may also be an effective adjunctive therapy to improve the outcome after ischemic stroke before or concurrently with reperfusion therapy such as thrombolysis or thrombectomy.

As a tPA inhibitor, neuroserpin alleviates brain damage caused by prolonged treatment of tPA thrombolysis in MCAO rat models (Zhang et al., 2002; Cai et al., 2020). Whether the protective effect of neuroserpin is via inhibiting endogenous tPA is still unclear. A previous study showed that the interaction between neuroserpin and tPA is unstable, with a short-lived and reversible nature (Barker-Carlson et al., 2002). Moreover, neuroserpin shows retained protective effects against I/R injury in tPA-deficient mice and neurons (Wu et al., 2010; Ma et al., 2012; Gu et al., 2015). Neuroserpin is a widely-studied neuroprotective secreted protein, but whether its secretion is altered during I/R has not been explored. We showed here that secreted neuroserpin was drastically decreased in I/R-injured cortical neurons and mice, which may be from the dysfunctional secretory pathway under ER stress. Conditional medium from normal neurons exerted a protective effect in OGD/R neurons. While multiple neuroprotective agents are secreted by neurons, such as brain-derived neurotrophic factor, we demonstrated that secreted neuroserpin is essential for neuroprotection, as the protective effect of the conditioned medium was diminished by neutralizing neuroserpin using a

specific antibody. Our result is consistent with the clinical findings that higher serum neuroserpin levels are associated with a smaller infarct volume and better outcome of patients (Rodríguez-González et al., 2011c; Wu et al., 2017), supporting the notion that depletion of extracellular neuroserpin contributes to the pathophysiology of neuronal damage by I/R. This explains why supplying exogenous extracellular recombinant neuroserpin in the ischemic brain or neurons is effective for neuroprotection (Yepes et al., 2000; Cinelli et al., 2001; Zhang et al., 2002; Wu et al., 2010; Rodríguez-González et al., 2011a; Ma et al., 2012; Gu et al., 2015; Yang et al., 2016; Cai et al., 2020). In our study, we demonstrated that early administration of exogenous neuroserpin effectively attenuated the activation of the initial ER sensor and inhibition of protein synthesis and reduced the subsequent signaling transduction of ER stress-induced apoptosis. Moreover, pharmacological activation of ER stress canceled the neuroprotection of neuroserpin both *in vitro* and *in vivo*, suggesting that the neuroprotection of neuroserpin is dependent on ER stress inhibition.

The mechanism of neuroserpin-mediated suppression of ER stress is still unclear; this is a limitation of this study and requires further investigation. An overload of cytoplasmic Ca<sup>2+</sup> levels caused by increased glutamate release is a common pathological change in ischemia. Notably, the serum neuroserpin level is negatively correlated with the glutamate level within the

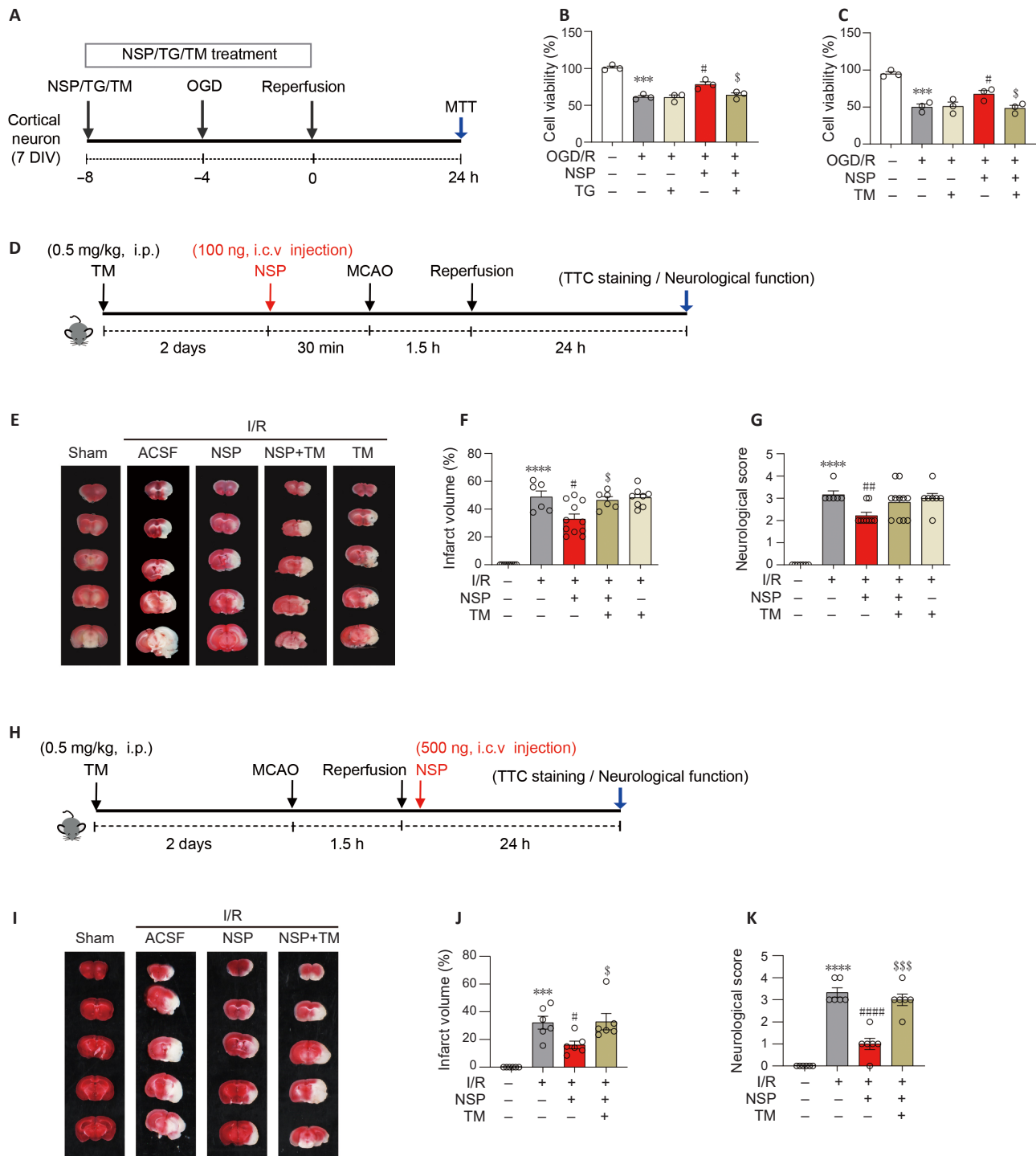


**Figure 5 | Neuroprotective effect of neuroserpin is dependent on the suppression of ER stress *in vitro* and *in vivo*.**

(A) Schematic representation of the timing of *in vitro* experimental procedures. NSP (20 ng/mL) with or without the ER stress activators TG (100 nM) or TM (50  $\mu$ M) was added to cultures of cortical neurons (7 DIV) 4 hours before OGD and during OGD, followed by reperfusion. (B, C) MTT assay was performed to determine OGD/R-injured neurons treated with NSP and TG (b) or TM (c) ( $n = 3$ ). \*\*\* $P < 0.001$ , OGD/R vs. control; # $P < 0.05$ , OGD/R + NSP vs. OGD/R; \$ $P < 0.05$ , OGD/R + NSP + TG/TM vs. OGD/R + NSP, unpaired *t*-test. (D) The schematic representation of the timing of *in vivo* experimental procedures. TM (0.5 mg/kg) was i.p. administered to adult mice 2 days before MCAO, and NSP (100 ng) was i.c.v injected 30 minutes before MCAO; MCAO lasted for 1.5 hours followed by reperfusion for 24 hours. (E) TTC-stained coronal brain slices from representative brains. (F) Quantitative analysis of infarct volumes ( $n = 9$  for sham group,  $n = 6$  for I/R group,  $n = 8$  for I/R + TM group,  $n = 11$  for I/R + NSP group,  $n = 6$  for I/R + NSP + TM group). \*\*\*\* $P < 0.0001$ , I/R vs. sham; # $P < 0.05$ , I/R + NSP vs. I/R; \$ $P < 0.05$ , I/R + NSP + TM vs. I/R + NSP, unpaired *t*-test. (G) Quantitative analysis of the neurological function by Zea-Longa test ( $n = 9$  for sham,  $n = 6$  for I/R,  $n = 7$  for I/R + TM,  $n = 9$  for I/R + NSP,  $n = 11$  for I/R + NSP + TM). \*\*\*\* $P < 0.0001$ , I/R vs. sham; ### $P < 0.01$ , I/R + NSP vs. I/R, unpaired *t*-test. (H) Schematic of the experimental procedure in which NSP was treated after MCAO. TM (0.5 mg/kg) was i.p. administered to adult mice 2 days before MCAO, and NSP (500 ng) was i.c.v injected immediately after ischemia. (I) TTC-stained coronal brain slices from representative brains. (J) Quantitative analysis of infarct volumes ( $n = 6$ ). \*\*\*\* $P < 0.001$ , I/R vs. Sham; # $P < 0.05$ , I/R + NSP vs. I/R; \$ $P < 0.05$ , I/R + NSP + TM vs. I/R + NSP, unpaired *t*-test. (K) Quantitative analysis of the neurological function by Zea-Longa test ( $n = 6$ ). \*\*\*\* $P < 0.0001$ , I/R vs. sham; ##### $P < 0.0001$ , I/R + NSP vs. I/R; \$\$\$ $P < 0.001$ , I/R + NSP + TM vs. I/R + NSP, unpaired *t*-test. All data are shown as mean  $\pm$  SEM. ACSF: Artificial cerebrospinal fluid; DIV: day *in vitro*; ER: endoplasmic reticulum; i.c.v: intracerebroventricular; i.p.: intraperitoneally; I/R: cerebral ischemia-reperfusion; MCAO: middle cerebral artery occlusion; MTT: 3-(4,5-dimethyl-2-thiazolyl)-2,5-diphenyl-2H-tetrazolium bromide; NSP: neuroserpin; OGD: oxygen-glucose deprivation; OGD/R: OGD/reperfusion; TG: thapsigargin; TM: thapsigargin; TTC: 2,3,5-triphenyl tetrazolium chloride.

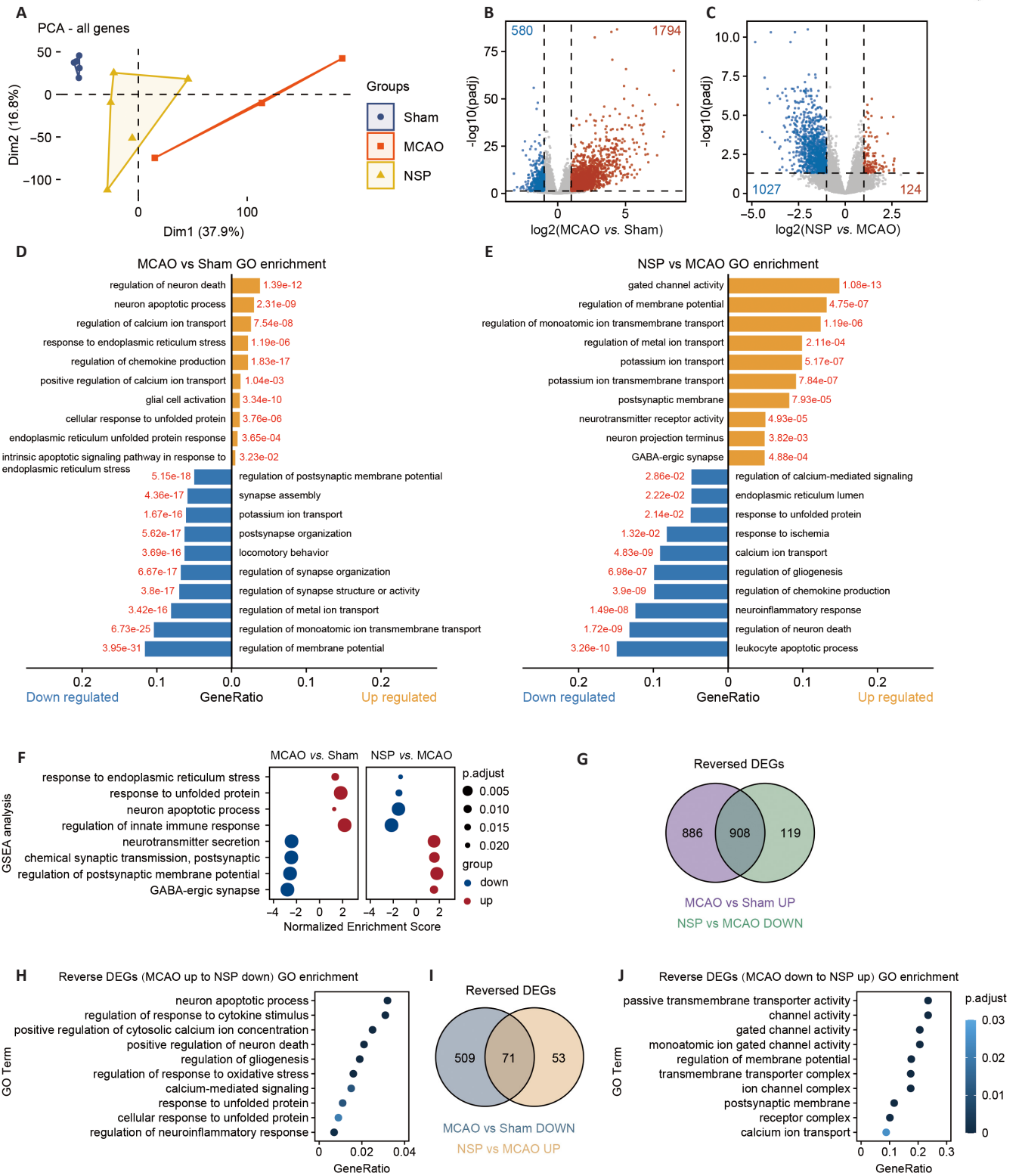


**Figure 6 | Transcriptomic analysis reveals that neuroserpin rescues ER stress and neuronal apoptosis in MCAO mice.**

(A) PCA of different groups (sham group,  $n = 5$ ; MCAO group,  $n = 3$ ; NSP treated group,  $n = 5$ ). (B) Volcano plots of DEGs between MCAO and sham groups (MCAO vs. sham). (C) Volcano plots of DEGs between NSP and MCAO groups (NSP vs. MCAO). For B and C, gray represents no significant change in expression, red represents upregulation, and blue represents downregulation. The dotted horizontal line represents an adjusted  $P$  value of 0.05. The dotted vertical line represents that fold change reaches 2-fold. (D) GO enrichment analysis of DEGs (MCAO vs. sham). (E) GO enrichment analysis of DEGs (NSP vs. MCAO). In D and E, the yellow and blue bars represent the selected enriched GO terms from the upregulated and downregulated DEGs, respectively. Bar length represents the gene ratio. Red numbers are the adjusted  $P$  values. (F) The dot plot shows the selected enriched gene sets by GSEA (MCAO vs. sham and NSP vs. MCAO). Dots in blue and red represent downregulated and upregulated gene sets, respectively. The size of dots represents the adjusted  $P$  value. (G, H) Venn diagram shows the genes that were reversely regulated by NSP. (G) Upregulated DEGs in MCAO but downregulated DEGs in NSP. (H) GO enrichment analysis of reversed DEGs from G. (I) Downregulated DEGs in MCAO and upregulated DEGs in NSP. (J) GO enrichment analysis of reversed DEGs from I. The color depth of dots represents the adjusted  $P$  value. DEGs: Differentially expressed genes; GO: gene ontology; GSEA: Gene Set Enrichment Analysis; MCAO: middle cerebral artery occlusion; NSP: neuroserpin; PCA: principal components analysis.

first 24 hours after ischemia (Rodríguez-González et al., 2011b). Treatment of neuroserpin decreases calcium influx mediated by N-methyl-D-aspartate receptor, thus inhibiting excitotoxicity-induced neuronal death (Lebeurrier et al., 2005). Whether neuroserpin has a role in regulating glutamate release and N-methyl-D-aspartate receptor function should be investigated in future studies. Moreover, neuroserpin also inhibits neuronal injury induced by oxidative stress (Cheng et al., 2017; Han et al., 2021a). Both  $Ca^{2+}$  dysregulation and oxidative stress may be triggers of ER stress and in turn exacerbated by ER stress. Indeed, our transcriptomic data revealed that in addition to causing changes in multiple ER stress-related pathways, neuroserpin treatment also leads to changes of calcium-mediated signaling and oxidative stress in the MCAO brain. Whether neuroserpin acts on these upstream damaging signals or directly on ER stress molecules is not yet clear. Moreover, Kondo et al. (2015) found co-localization of neuroserpin and the ER chaperone protein BiP in subplate neurons. As ER stress can be triggered by disassociation of BiP with ER stress sensors such as PERK and IRE1 (Chen et al., 2023b), it is worth investigating whether neuroserpin influences the interaction between BiP and ER stress sensors. The explorations of the above-mentioned questions are necessary to understand the specific molecular mechanism underlying the regulation of ER stress and neuroprotection by neuroserpin.

Overall, our findings demonstrate that ER stress is an early event triggered by ischemia, characterized by the initial acute activation of ER stress transmembrane sensors and inhibition of protein synthesis, followed by subsequent apoptotic responses. Administration of exogenous neuroserpin at early stages effectively reversed the ER stress-mediated signaling transduction, reduced neuronal death and cerebral infarction, and enhanced neurological function in I/R models. These results provide novel mechanisms of the neuroprotective properties of neuroserpin and underscore the potential of intervening ER stress with neuroserpin as a therapeutic strategy for ischemic stroke.

**Acknowledgments:** We thank Professor Wei Yang from Zhejiang University for coaching us the MCAO procedure, and we are grateful for the constructive suggestions from Prof. Masahiro Tsuji in Kyoto Women's University.

**Author contributions:** Study design and conception: LS, ZM, YL, and QZ; data collection: PL and LG; figure and table design and preparation: PL, ZH, and YP; manuscript writing: QZ, QS, and PZ; manuscript editing: YL, SZ, and WL; manuscript review: LS, ZM, XZ, NM, IA, YF, EK, and XQZ. All authors read and approved the final version of the manuscript.

**Conflicts of interest:** No potential conflicts of interest.

**Data availability statement:** All data relevant to the study are included in the article or uploaded as Additional files.

**Open access statement:** This is an open access journal, and articles are distributed under the terms of the Creative Commons Attribution-NonCommercial-ShareAlike 4.0 License, which allows others to remix, tweak, and build upon the work non-commercially, as long as appropriate credit is given and the new creations are licensed under the identical terms.

**Open peer reviewers:** Giovanna Galliciotti, University Medical Center Hamburg-Eppendorf, Germany; Nathan K Evanson, Cincinnati Children's Hospital Medical Center, USA.

**Additional files:**

**Additional Figure 1:** Quantification of the purity of cultured cortical neurons.

**Additional Figure 2:** The ER stress activator thapsigargin induces similar signaling transduction sequence as induced by OGD/R in cultured cortical neurons.

**Additional Figure 3:** 4-PBA and Sal treatment alone do not alter cell viability of cortical neurons.

**Additional Figure 4:** ER stress activators block the neuroprotection of NSP.

**Additional file 1:** Open peer review reports 1 and 2.

## References

Adorjan I, Tyler T, Bhaduri A, Demharter S, Finszter CK, Bako M, Sebok OM, Nowakowski TJ, Khodosevich K, Møllgård K, Kriegstein AR, Shi L, Hoerder-Suabedissen A, Ansgore O, Molnár Z (2019) Neuroserpin expression during human brain development and in adult brain revealed by immunohistochemistry and single cell RNA sequencing. *J Anat* 235:543-554.

Almanza A, et al. (2019) Endoplasmic reticulum stress signalling- from basic mechanisms to clinical applications. *FEBS J* 286:241-278.

Badiola N, Penas C, Miñano-Molina A, Barneda-Zahonero B, Fadó R, Sánchez-Opazo G, Comella JX, Sabriá J, Zhu C, Blomgren K, Casas C, Rodríguez-Alvarez J (2011) Induction of ER stress in response to oxygen-glucose deprivation of cortical cultures involves the activation of the PERK and IRE-1 pathways and of caspase-12. *Cell Death Dis* 2:e149.

Barker-Carlson K, Lawrence DA, Schwartz BS (2002) Acyl-enzyme complexes between tissue-type plasminogen activator and neuroserpin are short-lived in vitro. *J Biol Chem* 277:46852-46857.

Boyce M, Bryant KF, Jousse C, Long K, Harding HP, Scheuner D, Kaufman RJ, Ma D, Coen DM, Ron D, Yuan J (2005) A selective inhibitor of eIF2alpha dephosphorylation protects cells from ER stress. *Science* 307:935-939.

Cai L, Zhou Y, Wang Z, Zhu Y (2020) Neuroserpin extends the time window of tPA thrombolysis in a rat model of middle cerebral artery occlusion. *J Biochem Mol Toxicol* 34:e22570.

Campbell BCV, et al. (2019) Extending thrombolysis to 4-5-9 h and wake-up stroke using perfusion imaging: a systematic review and meta-analysis of individual patient data. *Lancet* 394:139-147.

Chen F, Liu J, Li FQ, Wang SS, Zhang YY, Lu YY, Hu FF, Yao RQ (2023a)  $\beta$ 2-Microglobulin exacerbates neuroinflammation, brain damage, and cognitive impairment after stroke in rats. *Neural Regen Res* 18:603-608.

Chen X, Shi C, He M, Xiong S, Xia X (2023b) Endoplasmic reticulum stress: molecular mechanism and therapeutic targets. *Signal Transduct Target Ther* 8:352.

Cheng Y, Loh YP, Birch NP (2017) Neuroserpin attenuates H(2)O(2)-induced oxidative stress in hippocampal neurons via AKT and BCL-2 signaling pathways. *J Mol Neurosci* 61:123-131.

Cinelli P, Madani R, Tsuzuki N, Vallet P, Arras M, Zhao CN, Osterwalder T, Rüllicke T, Sonderegger P (2001) Neuroserpin, a neuroprotective factor in focal ischemic stroke. *Mol Cell Neurosci* 18:443-457.

Ding S, Chen Q, Chen H, Luo B, Li C, Wang L, Asakawa T (2021) The neuroprotective role of neuroserpin in ischemic and hemorrhagic stroke. *Curr Neuropharmacol* 19:1367-1378.

Dobin A, Davis CA, Schlesinger F, Drenkow J, Zaleski C, Jha S, Batut P, Chaisson M, Gingeras TR (2013) STAR: ultrafast universal RNA-seq aligner. *Bioinformatics* 29:15-21.

Gao B, Zhang XY, Han R, Zhang TT, Chen C, Qin ZH, Sheng R (2013) The endoplasmic reticulum stress inhibitor salubrinal inhibits the activation of autophagy and neuroprotection induced by brain ischemic preconditioning. *Acta Pharmacol Sin* 34:657-666.

Gelderblom M, Neumann M, Ludewig P, Bernreuther C, Krasemann S, Arunachalam P, Gerloff C, Glatzel M, Magnus T (2013) Deficiency in serine protease inhibitor neuroserpin exacerbates ischemic brain injury by increased postischemic inflammation. *PLoS One* 8:e63118.

George PM, Steinberg GK (2015) Novel stroke therapeutics: unraveling stroke pathophysiology and its impact on clinical treatments. *Neuron* 87:297-309.

Godinez A, Rajput R, Chitranshi N, Gupta V, Basavarajappa D, Sharma S, You Y, Pushpitha K, Dhiman K, Mirzaei M, Graham S, Gupta V (2022) Neuroserpin, a crucial regulator for axogenesis, synaptic modelling and cell-cell interactions in the pathophysiology of neurological disease. *Cell Mol Life Sci* 79:172.

Gong L, Tang Y, An R, Lin M, Chen L, Du J (2017) RTN1-C mediates cerebral ischemia/reperfusion injury via ER stress and mitochondria-associated apoptosis pathways. *Cell Death Dis* 8:e3080.

Gong T, Wang Q, Lin Z, Chen ML, Sun GZ (2012) Endoplasmic reticulum (ER) stress inhibitor salubrinal protects against ceramide-induced SH-SY5Y cell death. *Biochem Biophys Res Commun* 427:461-465.

Gu RP, Fu LL, Jiang CH, Xu YF, Wang X, Yu J (2015) Retina is protected by neuroserpin from ischemic/reperfusion-induced injury independent of tissue-type plasminogen activator. *PLoS One* 10:e0130440.

Guo D, Peng Y, Wang L, Sun X, Wang X, Liang C, Yang X, Li S, Xu J, Ye WC, Jiang B, Shi L (2021) Autism-like social deficit generated by Dock4 deficiency is rescued by restoration of Rac1 activity and NMDA receptor function. *Mol Psychiatry* 26:1505-1519.

Han S, Zhang D, Dong Q, Wang X, Wang L (2021a) Deficiency in Neuroserpin Exacerbates CoCl(2) Induced hypoxic injury in the zebrafish model by increased oxidative stress. *Front Pharmacol* 12:632662.

Han Y, Yuan M, Guo YS, Shen XY, Gao ZK, Bi X (2021b) Mechanism of endoplasmic reticulum stress in cerebral ischemia. *Front Cell Neurosci* 15:704334.

Hu X, Wu L, Liu X, Zhang Y, Xu M, Fang Q, Lu L, Niu J, Abd El-Aziz TM, Jiang LH, Li F, Yang W (2021) Deficiency of ROS-activated TRPM2 channel protects neurons from cerebral ischemia-reperfusion injury through upregulating autophagy. *Oxid Med Cell Longev* 2021:7356266.

Kalogeris T, Baines CP, Krenz M, Korthuis RJ (2012) Cell biology of ischemia/reperfusion injury. *Int Rev Cell Mol Biol* 298:229-317.

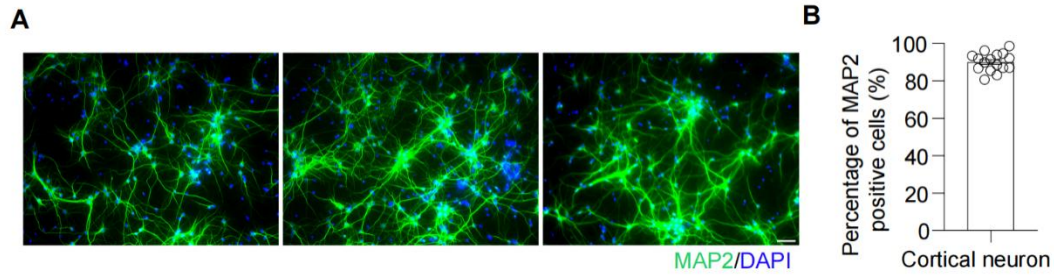
Kim JS, Heo RW, Kim H, Yi CO, Shin HJ, Han JW, Roh GS (2014) Salubrinal, ER stress inhibitor, attenuates kainic acid-induced hippocampal cell death. *J Neural Transm (Vienna)* 121:1233-1243.

Krueger SR, Ghisu GP, Cinelli P, Gschwend TP, Osterwalder T, Wolfer DP, Sonderegger P (1997) Expression of neuroserpin, an inhibitor of tissue plasminogen activator, in the developing and adult nervous system of the mouse. *J Neurosci* 17:8984-8996.

Lebeurrier N, Liot G, Lopez-Atalaya JP, Orset C, Fernandez-Monreal M, Sonderegger P, Ali C, Vivien D (2005) The brain-specific tissue-type plasminogen activator inhibitor, neuroserpin, protects neurons against excitotoxicity both in vitro and in vivo. *Mol Cell Neurosci* 30:552-558.

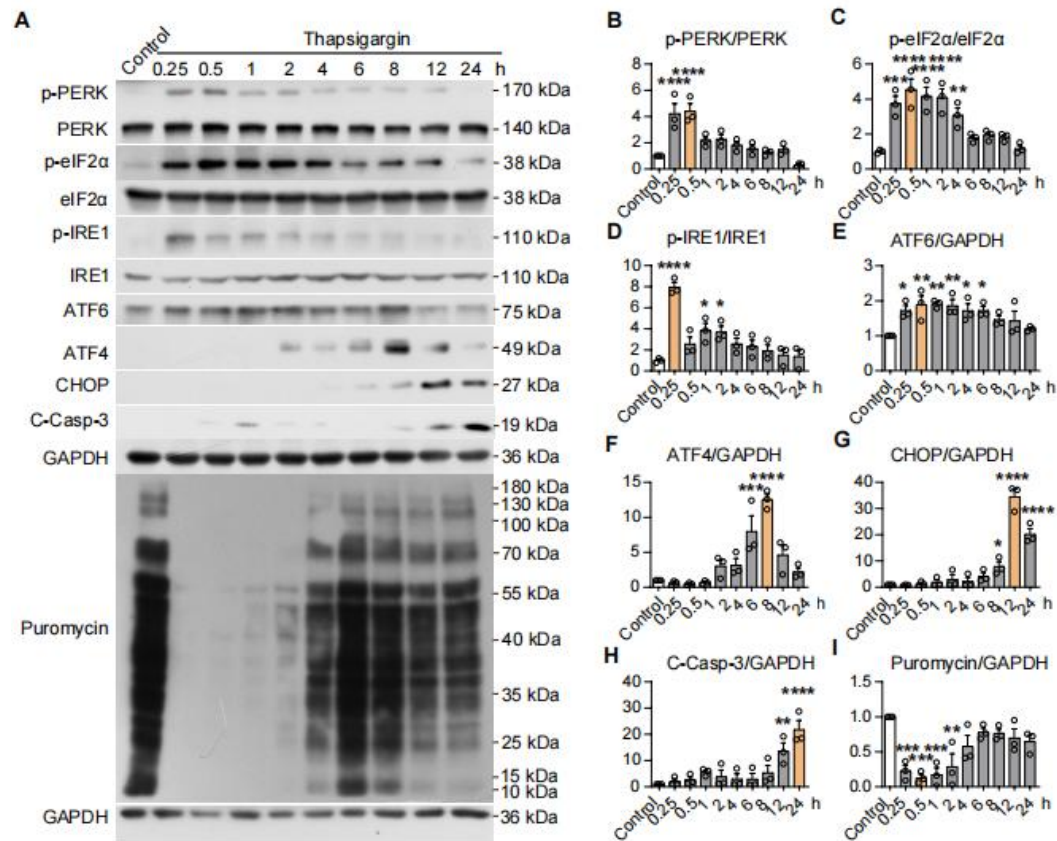
- Lee JM, Grabb MC, Zipfel GJ, Choi DW (2000) Brain tissue responses to ischemia. *J Clin Invest* 106:723-731.
- Lee TW, Tsang VW, Loef EJ, Birch NP (2017) Physiological and pathological functions of neuroserpin: Regulation of cellular responses through multiple mechanisms. *Semin Cell Dev Biol* 62:152-159.
- Li Y, Li M, Feng S, Xu Q, Zhang X, Xiong X, Gu L (2024) Ferroptosis and endoplasmic reticulum stress in ischemic stroke. *Neural Regen Res* 19:611-618.
- Liao Y, Zhuang X, Huang X, Peng Y, Ma X, Huang ZX, Liu F, Xu J, Wang Y, Chen WM, Ye WC, Shi L (2018) A bivalent securinine compound SN3-L6 induces neuronal differentiation via translational upregulation of neurogenic transcription factors. *Front Pharmacol* 9:290.
- Liao Y, Wang JY, Pan Y, Zou X, Wang C, Peng Y, Ao YL, Lam MF, Zhang X, Zhang XQ, Shi L, Zhang S (2023) The protective effect of (-)-tetrahydroalstonine against OGD/R-induced neuronal injury via autophagy regulation. *Molecules* 28:2370.
- Liu C, Yang TH, Li HD, Li GZ, Liang J, Wang P (2023) Exosomes from bone marrow mesenchymal stem cells are a potential treatment for ischemic stroke. *Neural Regen Res* 18:2246-2251.
- Liu C, Ju R (2024) Potential role of endoplasmic reticulum stress in modulating protein homeostasis in oligodendrocytes to improve white matter injury in preterm infants. *Mol Neurobiol* doi: 10.1007/s12035-023-03905-8.
- Longa EZ, Weinstein PR, Carlson S, Cummins R (1989) Reversible middle cerebral artery occlusion without craniectomy in rats. *Stroke* 20:84-91.
- Love MI, Huber W, Anders S (2014) Moderated estimation of fold change and dispersion for RNA-seq data with DESeq2. *Genome Biol* 15:550.
- Luchetti F, Carloni S, Nasoni MG, Reiter RJ, Balduini W (2023) Melatonin, tunneling nanotubes, mesenchymal cells, and tissue regeneration. *Neural Regen Res* 18:760-762.
- Lv S, Geng X, Yun HJ, Ding Y (2023) Phenothiazines reduced autophagy in ischemic stroke through endoplasmic reticulum (ER) stress-associated PERK-eIF2 $\alpha$  pathway. *Exp Neurol* 369:114524.
- Ma J, Tong Y, Yu D, Mao M (2012) Tissue plasminogen activator-independent roles of neuroserpin in the central nervous system. *Neural Regen Res* 7:146-151.
- Ma X, Li L, Li Z, Huang Z, Yang Y, Liu P, Guo D, Li Y, Wu T, Luo R, Xu J, Ye WC, Jiang B, Shi L (2022) eEF2 in the prefrontal cortex promotes excitatory synaptic transmission and social novelty behavior. *EMBO Rep* 23:e54543.
- Mayer ML, Miller RJ (1990) Excitatory amino acid receptors, second messengers and regulation of intracellular Ca<sup>2+</sup> in mammalian neurons. *Trends Pharmacol Sci* 11:254-260.
- Millar LJ, Shi L, Hoerder-Suabedissen A, Molnár Z (2017) Neonatal hypoxia ischaemia: mechanisms, models, and therapeutic challenges. *Front Cell Neurosci* 11:78.
- Nakka VP, Gusain A, Raghubir R (2010) Endoplasmic reticulum stress plays critical role in brain damage after cerebral ischemia/reperfusion in rats. *Neurotox Res* 17:189-202.
- National Institute of Neurological Disorders and Stroke rt-PA Stroke Study Group (1995) Tissue plasminogen activator for acute ischemic stroke. *N Engl J Med* 333:1581-1587.
- Pan YW, Wu DP, Liang HF, Tang GY, Fan CL, Shi L, Ye WC, Li MM (2022) Total saponins of panax notoginseng activate Akt/mTOR pathway and exhibit neuroprotection in vitro and in vivo against ischemic damage. *Chin J Integr Med* 28:410-418.
- Percie du Sert N, et al. (2020) The ARRIVE guidelines 2.0: Updated guidelines for reporting animal research. *PLoS Biol* 18:e3000410.
- Qian XH, Liu XL, Chen G, Chen SD, Tang HD (2022) Injection of amyloid- $\beta$  to lateral ventricle induces gut microbiota dysbiosis in association with inhibition of cholinergic anti-inflammatory pathways in Alzheimer's disease. *J Neuroinflammation* 19:236.
- Rodríguez-González R, Agulla J, Pérez-Mato M, Sobrino T, Castillo J (2011a) Neuroprotective effect of neuroserpin in rat primary cortical cultures after oxygen and glucose deprivation and tPA. *Neurochem Int* 58:337-343.
- Rodríguez-González R, Sobrino T, Rodríguez-Yáñez M, Millán M, Brea D, Miranda E, Moldes O, Pérez J, Lomas DA, Leira R, Dávalos A, Castillo J (2011b) Association between neuroserpin and molecular markers of brain damage in patients with acute ischemic stroke. *J Transl Med* 9:58.
- Rodríguez-González R, Millán M, Sobrino T, Miranda E, Brea D, de la Ossa NP, Blanco M, Perez J, Dorado L, Castellanos M, Lomas DA, Moro MA, Dávalos A, Castillo J (2011c) The natural tissue plasminogen activator inhibitor neuroserpin and acute ischaemic stroke outcome. *Thromb Haemost* 105:421-429.
- Roussel BD, Kruppa AJ, Miranda E, Crowther DC, Lomas DA, Marciniak SJ (2013) Endoplasmic reticulum dysfunction in neurological disease. *Lancet Neurol* 12:105-118.
- Satapathy S, Wilson MR (2023) Roles of constitutively secreted extracellular chaperones in neuronal cell repair and regeneration. *Neural Regen Res* 18:769-772.
- Schneider CA, Rasband WS, Eliceiri KW (2012) NIH Image to ImageJ: 25 years of image analysis. *Nat Methods* 9:671-675.
- Sharma D, Singh JN, Sharma SS (2016) Effects of 4-phenyl butyric acid on high glucose-induced alterations in dorsal root ganglion neurons. *Neurosci Lett* 635:83-89.
- Shi Q, Zhang Q, Peng Y, Zhang X, Wang Y, Shi L (2019) A natural diarylheptanoid protects cortical neurons against oxygen-glucose deprivation-induced autophagy and apoptosis. *J Pharm Pharmacol* 71:1110-1118.
- Sokka AL, Putkonen N, Mudo G, Pryazhnikov E, Reijonen S, Khiroug L, Belluardo N, Lindholm D, Korhonen L (2007) Endoplasmic reticulum stress inhibition protects against excitotoxic neuronal injury in the rat brain. *J Neurosci* 27:901-908.
- Srinivasan K, Sharma SS (2011) Sodium phenylbutyrate ameliorates focal cerebral ischemic/reperfusion injury associated with comorbid type 2 diabetes by reducing endoplasmic reticulum stress and DNA fragmentation. *Behav Brain Res* 225:110-116.
- Tang X, Yan T, Wang S, Liu Q, Yang Q, Zhang Y, Li Y, Wu Y, Liu S, Ma Y, Yang L (2024) Treatment with  $\beta$ -sitosterol ameliorates the effects of cerebral ischemia/reperfusion injury by suppressing cholesterol overload, endoplasmic reticulum stress, and apoptosis. *Neural Regen Res* 19:642-649.
- Thiebaut AM, Hedou E, Marciniak SJ, Vivien D, Roussel BD (2019) Proteostasis during cerebral ischemia. *Front Neurosci* 13:637.
- Walter P, Ron D (2011) The unfolded protein response: from stress pathway to homeostatic regulation. *Science* 334:1081-1086.
- Wang L, Liu Y, Zhang X, Ye Y, Xiong X, Zhang S, Gu L, Jian Z, Wang H (2022) Endoplasmic reticulum stress and the unfolded protein response in cerebral ischemia/reperfusion injury. *Front Cell Neurosci* 16:864426.
- Wu J, Echeverry R, Guzman J, Yepes M (2010) Neuroserpin protects neurons from ischemia-induced plasmin-mediated cell death independently of tissue-type plasminogen activator inhibition. *Am J Pathol* 177:2576-2584.
- Wu T, Hu E, Xu S, Chen M, Guo P, Dai Z, Feng T, Zhou L, Tang W, Zhan L, Fu X, Liu S, Bo X, Yu G (2021) clusterProfiler 4.0: A universal enrichment tool for interpreting omics data. *Innovation (Camb)* 2:100141.
- Wu W, Asakawa T, Yang Q, Zhao J, Lu L, Luo Y, Gong P, Han S, Li W, Namba H, Wang L (2017) Effects of neuroserpin on clinical outcomes and inflammatory markers in Chinese patients with acute ischemic stroke. *Neurol Res* 39:862-868.
- Wu Z, Yang F, Jiang S, Sun X, Xu J (2018) Induction of liver steatosis in BAP31-deficient mice burdened with tunicamycin-induced endoplasmic reticulum stress. *Int J Mol Sci* 19:2291.
- Xin Q, Ji B, Cheng B, Wang C, Liu H, Chen X, Chen J, Bai B (2014) Endoplasmic reticulum stress in cerebral ischemia. *Neurochem Int* 68:18-27.
- Yang X, Asakawa T, Han S, Liu L, Li W, Wu W, Luo Y, Cao W, Cheng X, Xiao B, Namba H, Lu C, Dong Q, Wang L (2016) Neuroserpin protects rat neurons and microglia-mediated inflammatory response against oxygen-glucose deprivation- and reoxygenation treatments in an in vitro study. *Cell Physiol Biochem* 38:1472-1482.
- Yepes M, Sandkvist M, Wong MK, Coleman TA, Smith E, Cohan SL, Lawrence DA (2000) Neuroserpin reduces cerebral infarct volume and protects neurons from ischemia-induced apoptosis. *Blood* 96:569-576.
- Zhang Z, Zhang L, Yepes M, Jiang Q, Li Q, Arniogo P, Coleman TA, Lawrence DA, Chopp M (2002) Adjuvant treatment with neuroserpin increases the therapeutic window for tissue-type plasminogen activator administration in a rat model of embolic stroke. *Circulation* 106:740-745.
- Zhang ZB, Xiong LL, Xue LL, Deng YP, Du RL, Hu Q, Xu Y, Yang SJ, Wang TH (2021) MiR-127-3p targeting C1SD1 regulates autophagy in hypoxic-ischemic cortex. *Cell Death Dis* 12:279.
- Zhao H, Wang M, Huang X, Wu X, Xiao H, Jin F, Lv J, Cheng J, Zhao Y, Zhang C (2022) Wasp venom from *Vespa magnifica* acts as a neuroprotective agent to alleviate neuronal damage after stroke in rats. *Pharm Biol* 60:334-346.

C-Editor: Zhao M; S-Editors: Yu J, Li CH; L-Editors: Wolf GW, Song LP; T-Editor: Jia Y



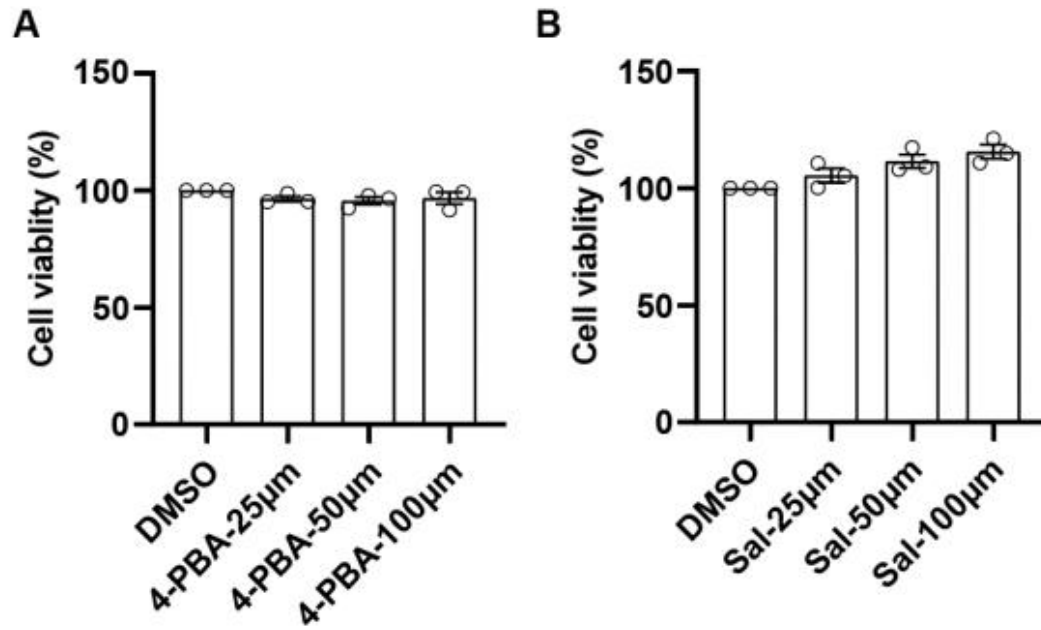
**Additional Figure 1 Quantification of the purity of cultured cortical neurons.**

(A) Representative images of MAP2 (neuronal marker, green, Alexa Fluor 488) and DAPI (blue) in 7 DIV cultured primary cortical neurons from three independent experiments. Scale bar: 50  $\mu$ m. (B) Quantification of the percentage of MAP2-positive cells. Data are shown as mean  $\pm$  SEM ( $n = 16$  views from three independent experiments (5–6 views from each experiment)). DAPI: 4',6-Diamidino-2-phenylindole; DIV: day in vitro; MAP2: microtubule-associated protein 2.



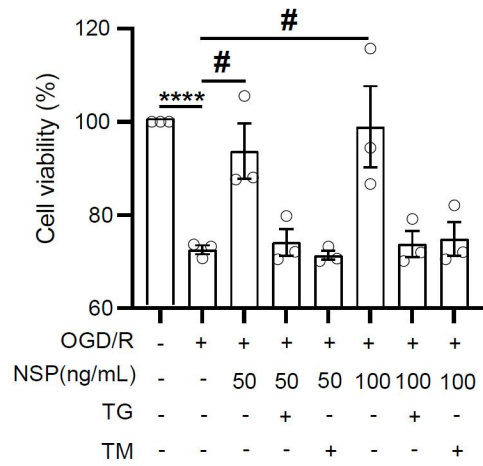
**Additional Figure 2 The ER stress activator thapsigargin induces similar signaling transduction sequence as induced by OGD/R in cultured cortical neurons.**

(A) Cultures of cortical neurons (7 DIV) were treated with thapsigargin (100 nM) for different time periods, and cell lysates were collected for western blot analysis. Representative western blots showing the levels of ER stress sensors, protein synthesis, and apoptosis-related proteins. (B–I) The normalized levels of p-PERK/PERK (B), p-eIF2α/eIF2α (C), p-IRE1/IRE1 (D), ATF6/GAPDH (E), puromycin/GAPDH (F), ATF4/GAPDH (G), CHOP/GAPDH (H), and cleaved caspase-3/GAPDH (I) ( $n = 3$ ). \* $P < 0.05$ , \*\* $P < 0.01$ , \*\*\* $P < 0.001$ , \*\*\*\* $P < 0.0001$ , vs. control, one-way analysis of variance followed by Dunnett's multiple comparison test. Data are shown as mean  $\pm$  SEM. ATF: Activating transcription factor; C-Casp-3: cleaved caspase-3; CHOP: CCAAT/enhancer binding protein homologous protein; DIV: day in vitro; eIF2α: eukaryotic translation initiation factor 2α; ER: endoplasmic reticulum; GAPDH: glyceraldehyde-3-phosphate dehydrogenase; IRE1: inositol requiring enzyme 1; OGD/R: oxygen-glucose deprivation/reperfusion; p-: phosphorylated-; PERK: double-stranded RNA-activated protein kinase-like ER kinase.



**Additional Figure 3 4-PBA and Sal treatment alone do not alter cell viability of cortical neurons.**

(A, B) Cell viability of neurons treated with 4-PBA (A) and Sal (B) of different concentrations (25, 50 or 100 μM) ( $n = 3$ ). Data are shown as mean  $\pm$  SEM. 4-PBA: Sodium 4-phenylbutyrate; DMSO: dimethyl sulfoxide; Sal: salubrinal.



**Additional Figure 4 ER stress activators block the neuroprotection of NSP.**

Cell viability of neurons treated with 50 or 100 ng/mL NSP in the presence or absence of ER stress activators TG (100 nM) or TM (50  $\mu$ M) ( $n = 3$ ). \*\*\*\* $P < 0.0001$ , OGD/R vs. control; # $P < 0.05$ , OGD/R + NSP vs. OGD/R. Data are shown as mean  $\pm$  SEM. ER: Endoplasmic reticulum; NSP: neuroserpin; OGD/R: oxygen-glucose deprivation/reperfusion; TG: thapsigargin; TM: tunicamycin.